DEVELOPMENT OF THE CAPTIVE AEROSOL GROWTH AND EVOLUTION CHAMBER SYSTEM

A Thesis

by

CARLOS GABRIEL ANTONIETTI

Submitted to the Office of Graduate and Professional Studies of
Texas A&M University
in partial fulfillment of the requirements for the degree of

MASTER OF SCIENCE

Chair of Committee,	Donald R. Collins
Co-Chair of Committee,	Sarah D. Brooks
Committee Member,	Simon N. North
Head of Department,	Ping Yang

December 2014

Major Subject: Atmospheric Sciences

ABSTRACT

The Captive Aerosol Growth and Evolution (CAGE) Chamber System is an tool designed to study the evolution of aerosols under conditions identical or similar to those of the surrounding environment. Our motivation was to quantify the sensitivity of particle growth rate to trace gas concentrations, oxidants, other particles, and cloud processing. The main objective was to design a pair of transparent, chemically inert, and rotating chambers capable of withstanding a vacuum reflective of typical cloud-top pressures. Aerosol samples taken from the chambers are directed into a suite of instrumentation to study the physical and chemical properties of the evolving aerosol.

The chamber system is mounted on a field-deployable trailer through a rotating frame that tracks the sun. Each chamber consists of a set of three concentric thin film cylinders. On both ends of each chamber are inlets and outlets connected through rotary unions for control of trace gas and particle concentrations in the reactor volumes, which rotate about horizontal axes to extend particle retention time. The cylindrical chamber walls are made of transparent FEP Teflon that is both chemically inert and largely transparent for natural solar radiation that drives photo-oxidation processes. The reactor cylinder end walls are made of a permeable Teflon membrane for gas exchange between the inside of the chamber and pre-conditioned or filtered ambient gas. This continuous gas exchange permits dynamic control of the chamber composition without the particle dilution that would accompany a flow-through design. The gas composition in the

chambers can be varied for different experimental objectives. Controlled pressure differentials between the concentric volumes are designed to keep the walls semi-rigid during an experiment, while the outermost wall and high strength metal support frame withstand the vacuum in the chambers relative to surrounding air that becomes quite large during cloud formation cycles.

The CAGE system was first deployed during September and October 2012 at the Army Research Laboratory outside of Washington D.C. where basic functionalities were tested and experiments conducted to assess the rate at which bioaerosol properties and viability change in ambient air. Daily experiments lasted up to 7 hours, with both chambers rotating at 1 rpm and the platform rotating to track the sun. Injection of two different aerosol types with nearly monodisperse size distribution was followed by intermittent measurement and collection of those captive particles. The gas exchanged with one chamber was first scrubbed and filtered to provide a baseline for comparison while particle-filtered ambient air was exchanged with the other chamber. Preliminary results indicate that single particle fluorescence spectra vary both over time and with differing gas composition.

DEDICATION

To my wife Nazarena and children Rosario, Donato and Juana.

ACKNOWLEDGEMENTS

Although my name is on the cover of this manuscript the instrument described was possible by the joint effort of many. I would like to thank Dr. Collins for involving me in his research group and the exposure to design, build, re-design and re-build until desired performance is achieved of an instrument from zero. This instrument was designed by Dr. Collins with highly restrictive constraint on materials to use and demanding performance that took the collaboration of our entire research group, brainstorming and resources to build it. Special thanks to my co-workers Chance Spencer, Nathan Taylor and Jill Matus who brought ideas to design parts, found supplier and companies to do metal work and machining, wrote software and assembled the rest of the modules and instrument together. My participation was mainly on designing and building the Gas Exchange System, writing parts of the control software, adjusting and testing different components and to assemble it. The undergraduate student workers Samantha Wills, Erik Nielsen, Rob Navarro, Hannah Knight, Mindy Nicewonger, Hannah Uptown and Mark Benoit worked many hours throw-out the project. I am thankful for Mr. William Seward from the Chemistry Department Machine Shop provided assistance in the design and manufacturing process of key components and made several pieces. I would like to thank my advisory committee, Dr. Sarah Brooks and Dr. Simon North, for reviewing manuscript. The instrument was run for the first during a field project in the fall of 2012 at the Army Research Lab in Adelphi, MD. Thanks to Yong-Le Pan, Steve Hill and Mark Coleman from the US Army Research

Laboratory; Shanna Ratnesar-Shumate, Christopher Bare and Sean Kinahan from the Johns Hopkins University Applied Physics Laboratory and Andres Sanchez, Crystal Reed and Joshua Santarpia from Sandia National Laboratories for their assistance and collaboration in setting up our instrument.

Nathan Frank Taylor became my room-mate, office-mate and bbq-mate with whom I spent many hours discussing about the instruments but also life. His friendship made my graduate studies away from home and family manageable.

I am grateful to my parents for supporting my wife and kids in my home country during my time in Texas.

I am indebted for life to my wife for her patience and understanding.

TABLE OF CONTENTS

LIST OF FIGURES

1. INTRODUCTION

Aerosol particles suspended in the atmosphere undergo physical and chemical processes between their formation or emission and their eventual removal. During their lifetime, interaction with the surrounding environment determines how their properties will change, which in turn affects their lifetime. Aerosol research is largely motivated by several links to the radiation budget that determines global climate and by concerns about visibility degradation and urban and regional scale issues related to air quality and health effects. Atmospheric aerosols scatter and absorb light, thereby affecting atmospheric transmission of radiation and the overall planetary albedo. Additionally, aerosols are essential for cloud formation, as first observed by Aitken (1880a; 1880b) using an expansion chamber in which cloud condensation nuclei (CCN) activated to form droplets.

The 2007 Intergovernmental Panel on Climate Change (IPCC) report identifies a large uncertainty for the indirect effect aerosols have on climate in which pollution aerosol results in a higher concentration of droplets that share the same amount of liquid water, resulting in more reflective clouds and reduced transmission of sunlight to the surface where it would likely be absorbed. Further, cloud lifetime may be increased by the precipitation efficiency reduction that results from slower collision coalescence processes between smaller cloud particles.

The subset of an aerosol that can participate in these important cloud processes is determined by the link between aerosol particle chemical and physical properties and water vapor condensation described by Köhler theory.

The traditional Köhler equation that was first published over 70 years ago has recently been modified to better reflect the behavior of the complex chemical mixtures typically present in atmospheric particles. However, while these advances in understanding and treatment of particle activation improve predictability of cloud features such as droplet concentration, the computational complexity that results precludes use in global models that are ultimately the tools used to assess the link between changes in emissions of particles and their precursors and changes in temperature and precipitation.

The conversion of an emitted or nucleated aerosol particle into a CCN is parameterized in global models to reduce calculation time, leading to output uncertainties. Parameterization improvement is achieved by better knowledge of the activation behavior of common types of aerosols. One fundamental classification for this purpose is primary organic aerosol (POA), which is emitted directly into the atmosphere, while secondary organic aerosol (SOA) is formed by atmospheric reactions and subsequent gas to particle conversion. The source of both types of organic aerosol (OA) can be natural or anthropogenic, with particular interest in anthropogenic aerosols stemming from the ability to reduce their atmospheric concentration. Aerosol types are further separated into groups representative of major components and sources, e.g., hydrocarbon-like organic aerosol (HOA), oxygenated organic aerosol (OOA), biogenic

secondary organic aerosol (BSOA), and biomass burning organic aerosol (BBOA). Particles within each of these groups have different activation efficiencies that must be included in the models.

During transport, exposure to reactive and condensing atmospheric gases results in continual changes in aerosol properties and composition, with production of species among the 10,000 to 100,000 believed to exist in the atmosphere (Goldstein and Galbally, 2007). Within the volatile organic compound (VOC) gases, biogenics (BVOCs) emitted by many types of trees and plants can undergo 10^5~10^6 reactions (Hallquist et al., 2009). Isoprene (2-methyl-1,3butadiene) is an important and extensively studied BVOC that reacts rapidly with oxidants such as $OH\cdot$ and $NO_3\cdot$, resulting in several thousand products (Fan and Zhang, 2004).

Because of the wide variability of components in the aerosol and gas phase and the interactions among them, aerosol chemistry is often best studied with environmental chambers mimicking atmospheric conditions while allowing control of certain components of the experiment. Laboratory environmental or smog chambers are typically designed inside buildings with temperature control systems and artificial lights to produce the UV wavelengths of the solar spectrum, though some are instead located outside and exposed to natural sunlight. The internal volume for chambers in use around the world ranges from 1 to 270 m^3. Experiments are carried out in batch mode or with continuous flows. Studies using these chambers have provided much of the current understanding of SOA formation from VOC oxidation (Hallquist et al. 2009). One of the problems associated with environmental chamber experiments is that the time scales of

chemical reactions and aerosol processing are limited by particle loss by gravitational settling and deposition to the walls. The requisite injection of higher concentrations of reactive gases than those found naturally results in discrepancies between real conditions, models, and laboratory measurements.

One of the quantities describing the impact of aerosol exposure to gases is the particle diameter growth rate (GR), which reflects addition of mass. The GR of an aerosol has been measured by our group using a scanning mobility particle sizer (SMPS) and a humidified tandem differential mobility analyzer (H-TDMA). Detailed descriptions of the H-TDMA and a variant referred to as an ambient state TDMA (AS-TDMA) are given by Gasparini et al. (2006) and Taylor et al. (2011), respectively.

To quantify the GR of captive particles, our research group designed, built, and deployed a first generation chamber variant called the Ambient Aerosol Chambers for Evolution Studies (AACES). These portable, 1.2 m^3 chambers were constructed with transparent acrylic and FEP Teflon to allow penetration of natural sunlight and the photolysis reactions it drives. The chambers are partitioned into two volumes separated by an expanded polytetrafluoroethylene (ePTFE) membrane sheet across which there is bidirectional gas exchange, but no net dilution or particle exchange. The lower volume is referred to as the ambient exchange section while the larger upper volume is the reaction chamber. Several ports into both volumes are used for injection and sampling of aerosols and gases. Glen (2010) describes the results of several experiments conducted with the chambers in different locations in the U.S. to examine production and growth of SOA and aging of soot particles.

2. ENVIRONMENTAL CHAMBERS

2.1 Background

There are several facilities around the world that employ environmental or smog chambers to perform experiments that isolate the reactions and products for prescribed gas mixtures and environmental conditions. Most of these are indoor chambers that better enable repeatable experiments through control of temperature, relative humidity, and UV intensity. Temperature is typically controlled by large air conditioning systems and mapped by an array of thermistors.

Artificial lights such as black lights or argon or xenon arc lamps are used to generate typical daytime intensities of the portion of the UV spectrum that can penetrate the atmosphere and drive photochemistry near the ground. The emitted light spectrum is often monitored with a spectroradiometer to characterize any changes over time and to estimate the photolysis rates of several important compounds. The spectral profile is determined by the emission characteristics of the light sources and the transmission profiles of any optical filters, while intensity is usually controlled simply by altering the number of lights used. Lights are located some distance from the chamber walls to reduce undesirable temperature or intensity heterogeneity.

Before and after experiments, the Teflon chamber bags are typically flushed with zero air and then exposed to a high ozone concentration to remove background particles and gases inside the chambers and also to force wall off-gassing of compounds that

adsorb or absorb on the walls during experiments (Carter et al., 1995). The injected air is filtered by combinations of high-efficiency particulate absorption (HEPA) filters for particles, silica gel or drierite for water vapor, and a combination of media types such as activated alumina, molecular sieves, and activated charcoal for most reactive and oxidizing gases such as hydrocarbons, sulfur dioxide, nitrogen dioxide, nitric oxide, and ammonia. While flushing with zero air, lights are turned on to promote photo-oxidation and the chamber temperature elevated to increase off-gassing. Flushing and irradiation are usually continued until concentrations of key trace gases are below detection limits.

Several chamber facilities are active throughout the U.S. A few are described here as a basis for comparison and contrast with the design features of ours. The Carnegie Mellon University smog chamber consists of a 10~12 m^3 FEP Teflon bag suspended in an insulated and temperature controlled room. The chamber is surrounded by 64 GE F40BL UVA and 24 GE F20BL UVA black lights (Weitkamp et al., 2007).

The California Institute of Technology smog chamber facility consists of two 28 m^3 Teflon bags made out of 2 mil FEP. It has 300 Sylvania 350BL 40 W black lights. The bags are suspended side by side in a room and share injection and sampling lines that are alternated between the two using 3-way valves. There are two Teflon ports for gases and a stainless steel port for aerosol injection and withdrawal. The walls of the room are covered with UV-reflective aluminum panels. A 54 kW air conditioning system is used to control temperature in the range from 18°C to 50°C with lights on and 15°C to 50°C with lights off (Cocker et al., 2001). Experiments can last from 30 min to 24 h.

The Harvard Environmental Chamber (HEC) consists of a 5 m^3 Teflon bag made out of 2 mil PFA. The bag is suspended inside a room by a stainless steel frame. One side of the bag has ports for injection of aerosol and precursor gases and the opposite side has ports for sampling. It is surrounded by 48 Sylvania 350 BL 40 W black lights. The walls of the room are covered with reflective aluminum panels. During operation the inlet and outlet flow rates are matched.

The University of California at Riverside environmental chamber consists of two ~90 m^3 Teflon bags made out of 2 mil FEP. The chambers are illuminated by a 200 kW Argon arc lamp and/or 80 GE 350BL 115 W black lights. The room housing the chambers is continuously flushed with purified air and is covered with reflective aluminum panels. The eight inlet and outlet ports are located on the floor of the chamber and the accompanying gas and particle flows are routed to the next floor below in the building, where the instrumentation is located. The room temperature is adjustable between 5°C and 45°C by a 30 ton air conditioner unit. The top section of the support frame is moveable to allow expansion and contraction of the chamber. A Teflon coated fan inside the reactor premixes the volume before experiments start (Carter et al., 2005).

In Europe, universities and laboratories with smog chambers have formed the *Euro*pean simulation *cham*bers for investigating atmospheric *p*rocesses (Eurochamp-2) consortium that integrates research facilities in collaborative projects and supports cooperative projects between Germany, Spain, Ireland, France, Switzerland, United Kingdom, Sweden, and Denmark. Some goals are to have a central database, encourage data intercomparison and quality assurance, and facilitate development of common

techniques for inclusion of chamber experiment results in model development and evaluation (Eurochamp-2 proposal part B). The chamber network is currently the largest in the world. Some of the more research active facilities are described briefly here. The cylindrical SAPHIR chamber in Forschungszentrum Jülich, Germany has a diameter of 5 m and length of 18 m, with a resulting volume of 270 m^3. The facility includes instrumentation to directly measure radicals such as $OH\cdot$, $HO_2\cdot$, $RO_2\cdot$, and $NO_3\cdot$. Instrumentation is placed below the chamber floor inside a pair of containers.

The European photo reactor (Euphore) is a twin outdoor atmospheric simulation chamber facility in Spain. It has a half dome shape with a volume of ~200 m^3. It is made of 32 welded 0.13 mm FEP segments. The chamber floor is FEP lined aluminum that is refrigerated to maintain the same temperature as the surrounding air. It is operated at an overpressure of 100-200 Pa.

The Aerosol Interaction and Dynamics in the Atmosphere (AIDA) chamber is an 84.5 m^3 aluminum cylinder for aerosol and cloud particle experiments. An additional chamber of 3.9 m^3 volume made of stainless steel is used for aerosol injection. The chamber pressure can be controlled between 0.01 and 1000 hPa, the temperature between +50°C and -90°C, and the relative humidity between ~zero and supersaturation. It can be used for simulation of upper tropospheric and lower stratospheric conditions.

2.2 The 1st generation chambers

The Ambient Aerosol Chambers for Evolution Studies (AACES) were developed by our research group beginning in 2005. The design requirements for these field-deployable chambers were to produce an environment inside that mimics that immediately outside. Thus, gas phase composition, temperature, relative humidity, and UV and visible spectral intensity were not prescribed as with traditional chambers, but rather track ambient conditions. The final chambers are shown in Figure 1. Each chamber was constructed on a simple frame with wheels and several Teflon ports. The outer walls are made of UV-transparent acrylic and are lined on the inside by the inert FEP Teflon sheets. The chambers have two volumes, between which there is bidirectional gas exchange across a 2 mil expanded polytetrafluoroethylene (ePTFE) membrane sheet. This membrane is gas-permeable and non-reactive and has a fibrous structure that prevents transmission of particles. These white ePTFE membranes are easily seen in the chamber photo in Figure 1.

Figure 1. The first generation AACES chambers.

The upper reactor volume in the AACES chambers is about 1.2 m^3. The lower volume is the ambient gas exchange section through which ambient air pulled from a nearby elevated inlet is flushed. Several Teflon ports on both volumes are used for injection and sampling of aerosols and gases. Typical experiments are conducted by first injecting into the upper chamber a monodisperse, known composition, generated aerosol. Those captive particles are then exposed to trace gases and sunlight just as ambient particles would be in the surrounding air. Figure 2 shows the efficiency with which outside ozone penetrates into the reactor volume during an experiment in summer 2010

on top of the Oceanography and Meteorology building. The measurements were made by Peng, a student from Dr. Renyi Zhang from A&M Atmospheric Sciences department.

Observed particle chemical and physical changes are due to photo-oxidation and interaction with reactive and condensable gases. Results from extensive chamber characterization and from a series of research studies conducted at several U.S. sites are provided in Crystal Glen's Ph.D. dissertation (2010).

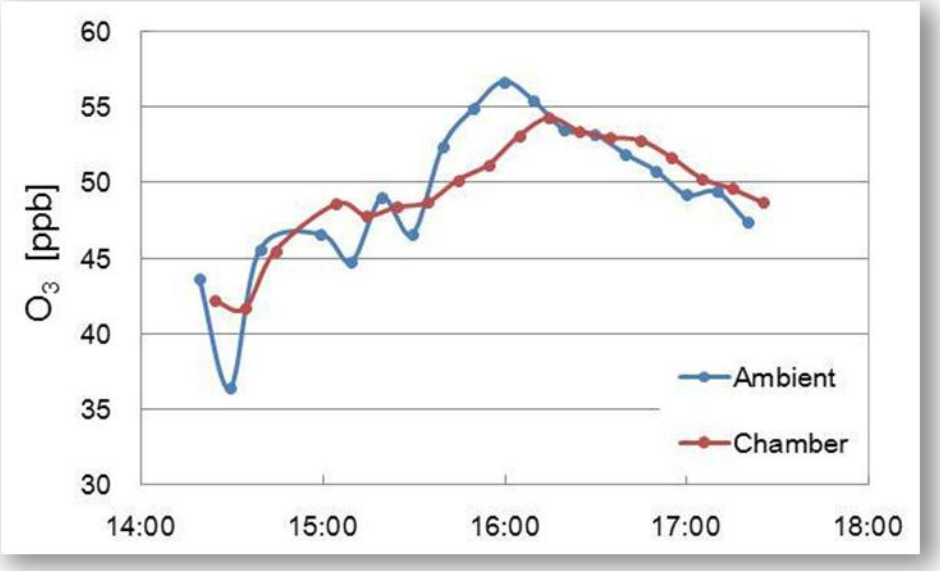

Figure 2. Ambient and reaction chamber ozone measurements (Peng, 2010).

2.3 Particle retention

Particle retention during chamber experiments is a major challenge because particle losses introduce uncertainty in calculated GR or aerosol mass production and may reduce particle measurement accuracy as signals approach noise levels. Chamber experiments are conducted either in continuous flow mode with balanced input and output flow rates or in batch mode in which all particle and gas injections are completed at the beginning of an experiment. For continuous mode operation, particles are injected and sampled at the same flow rate and the limiting particle residence time depends on the ratio of chamber volume to flow rate. The resulting residence time is often too short for experiments designed to study the slow evolution of particles undergoing ambient atmospheric processing. For this reason, seed particles are injected until a certain number concentration is reached, after which the chamber is isolated and samples are then taken at fixed intervals for the duration of the experiment. Figure 3 depicts different particle sizes that were introduced in the chamber by Dr. Collins's phD student Crystal Glen to measure the particle retention time with the 1st generation chamber. Further information can be found on Glen (2010) dissertation.

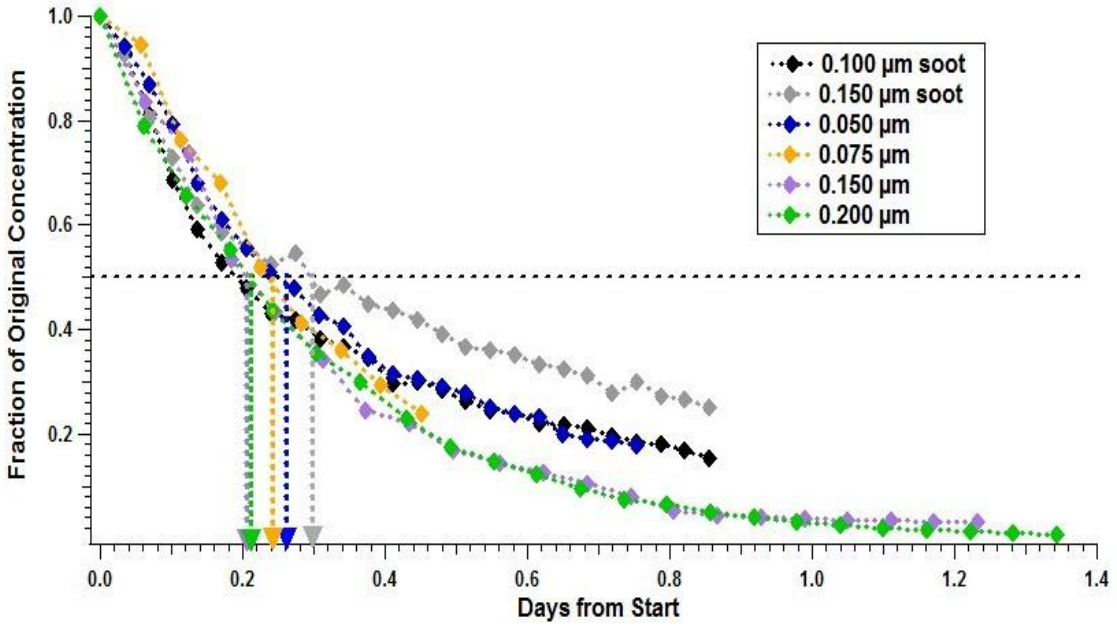

Figure 3. Particle retention time in the 1st generation chamber. Vertical dashed line indicates half-life. Glen, 2010

Particle concentration is constrained partly by losses to the chamber walls. Wall loss results from particle transport towards the walls by turbulent and Brownian diffusion, gravitational settling, and electrostatic drift.

Wall losses can be estimated by the wall loss coefficient, β, defined by Crump and Seinfeld (1981) for a spherical chamber as a function of chamber radius, particle diameter, particle Brownian diffusion coefficient, and turbulent diffusion rate represented by eddy diffusivity. The equation they present is derived neglecting convection due to thermal gradient. In the case where the chamber volume is not stirred

either by a fan or flow exchange, temperature homogeneity becomes important. Their equation applies to a sphere, where diffusion and sedimentation are coupled.

Chamber walls made out of Teflon acquire electrostatic charge that accelerates loss of charged seed particles. Simply injecting uncharged particles can help, but even those particles tend to acquire a Boltzmann charge equilibrium as gases in the chamber are ionized from cosmic rays and decay of radioactive gases such as Radon. To remove static charge an air stream with positive and negative ions is directed against the Teflon walls. Because of the construction design, acrylic is in contact with the FEP, which will generate static charge because the materials are at opposite end of the triboelectric series. For the 1st generation chamber, filtered air was directed through a ^{210}Po 200 μCi charging source and circulated inside the chamber and in between the acrylic frame and the outside of the reactor wall. The experience gained from this effort with the 1st generation chambers motivated construction of the aerosol classifier module on the aerosol generation cart (Section 3.6).

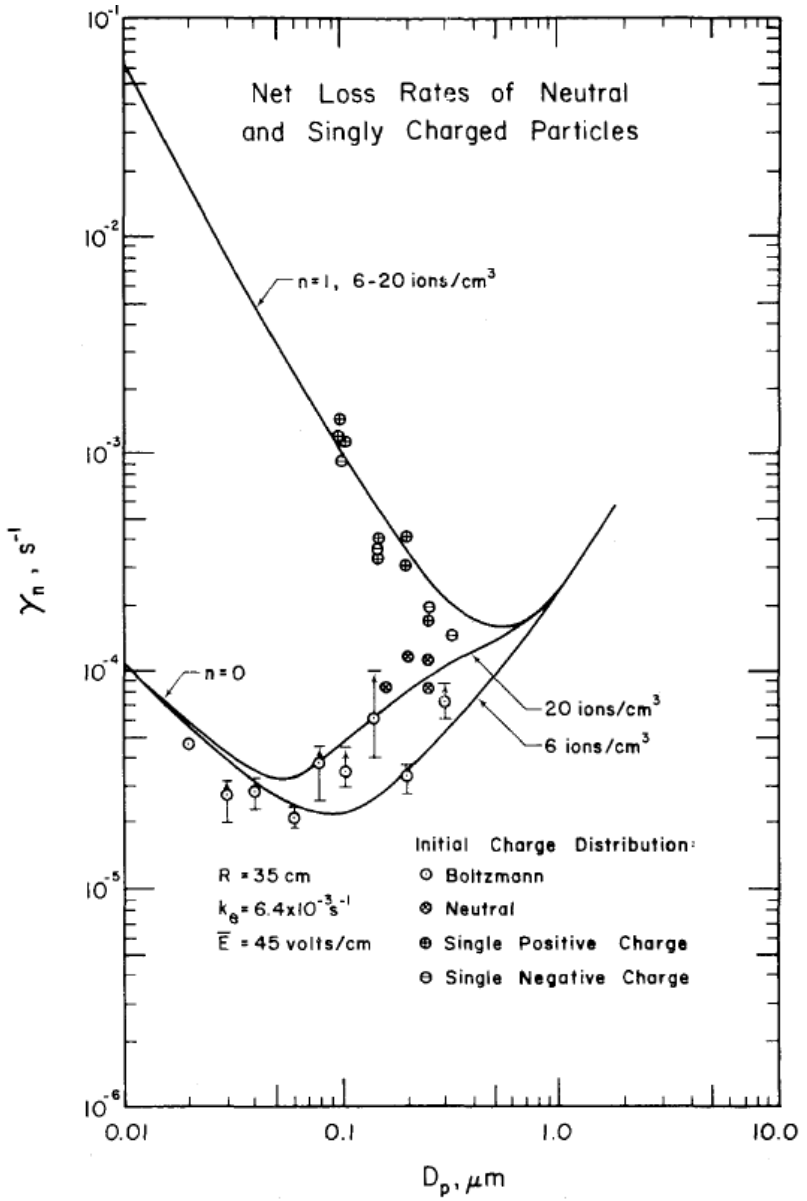

Figure 4. Wall loss for different charged particle states under different ion concentrations in a 250 liter Teflon bag. McMurry and Rader, 1985

From Figure 4 it is evident that loss of smaller particles is controlled by diffusion while that of larger particles results from gravitational settling. Particles between 0.1 and

1 μm are most sensitive to the influence of electric fields resulting from surface static charge. Particle loss rate can be minimized by distributing particles homogenously in the chamber, keeping temperature uniform to reduce convective mixing, neutralizing seed particles, and reducing electrostatic charge on the Teflon walls.

Because particle retention time is often short compared to time scales of atmospheric processing, higher concentrations of reactive gases are injected to accelerate reactions, resulting in atmospherically-unrealistic experimental conditions. The significant design modification of the 2nd generation chambers to permit slow rotation was motivated by the desire to enhance retention time. The technique is commonly used in the bioaerosol community, see Goldberg et al (1958), Gruel et al (1987) and Krumins et al (2008) .

2.4 Gas and particle mixing

Mixing techniques used with environmental chambers include use of Teflon coated fans inside the chamber, manually pushing the walls, and use of an external source of sonic waves. Regardless of approach, the objective is to achieve homogenous distributions of particles and gases inside the volume to reduce sampling biases, broadening of the particle size distribution, and spatially-varying chemical reaction rates. For the 1st generation chambers sonic waves were used to disrupt and mix the volume employing an external subwoofer with a 20Hz frequency audio signal feed, generating a pressure wave that mixes the particles and gases. For a scenario in which the volume is

well-mixed, the gas phase residence time can be estimated by dividing the total volume by the flushing flow rate. The sonic perturbation technique was tested with CO as a tracer gas. Gases were exchanged between the reaction chamber and the lower volume through which ambient air was continuously flushed. Carbon monoxide was injected into the ambient air flow and its concentration increased stepwise every 60 minutes. The observed upper volume response time constant was just over 30 min, which was only slightly longer than the limiting value for a well-mixed chamber for which there was no barrier between the upper and lower volumes. A similar response time was determined using variable humidity in the flushing flow.

A flow simulation was configured using CD ADAPCO's Star-CCM+ software to analyze flows and resulting particle distribution inside the chamber. The simulated chamber was a 1 m long by 0.8 m diameter cylinder oriented horizontally, with a resulting volume of 502 L.. It had 3/8" O.D. inlet and outlet ports on opposite sides. For the simulation, particles were injected at a rate sufficient to result in a mass concentration of 5 $\mu g/m^3$ following a 1-hr injection period. The inlet flow rate was fixed at 60 LPM and introduced 10 cm inside of the chamber wall. The introduced particle size and density were 1 µm and 1g cm^{-3}, respectively. The outlet flow conditions were: temperature 26.85ºC, pressure 101,325Pa, air density 1kg m^{-3}, and dynamic viscosity $1.85508x10^{-5}$ Pa s.

The steps taken in executing a CFD simulation are i) creation of a CAD model of physical equipment, ii) creation of geometry parts, iii) setup of a new region, iv) surface and volume mesh generation, v) selection of physical models to run, vi) specification of

boundary conditions, vii) preparation of different scenes to visualize the simulation results, and viii) running the simulation. To simulate this process I used a Lagrangian Multiphase Model, which represents a flow process that involves transport of liquid droplets within the fluid continuum. Figure 5 shows the flow velocity inside the chamber when the output is on a straight line with the input.

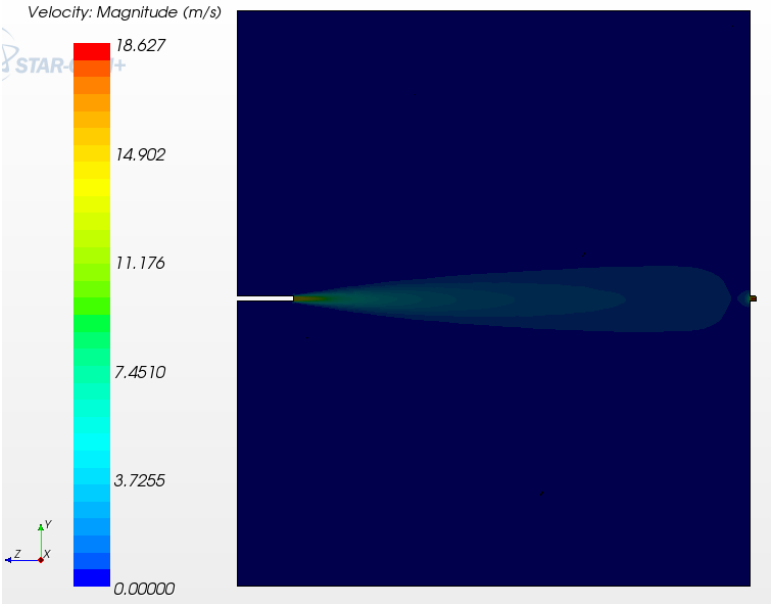

Figure 5. Flow field distribution on the plane section

Star-CCM+ has a Passive Scalar model to simulate the residence time (mean age of air) for a single phase that was used. A track file was added to the Lagrangian Multiphase Model to record variables linked with the parcel tracks. The parcel centroid, parcel index, particle residence time, and particle flow rate are saved in the track file. Figure 6 shows the particle residence time inside the chamber.

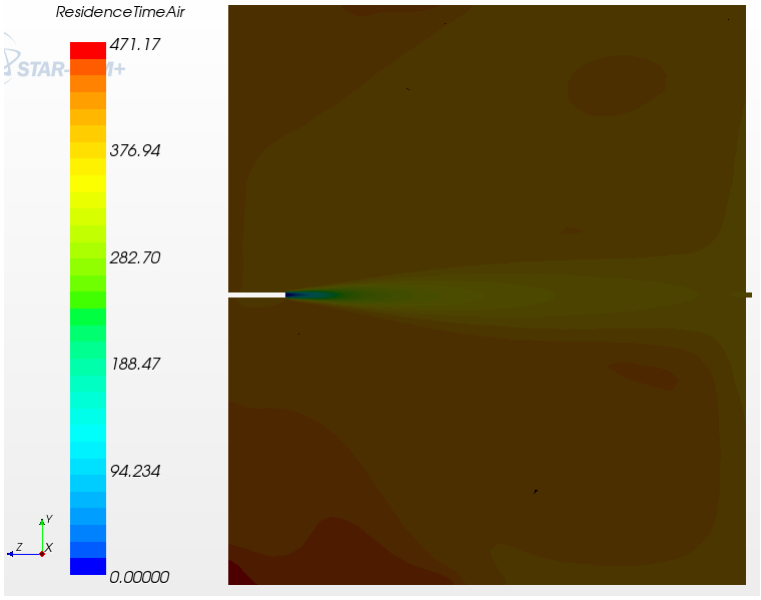

Figure 6. Air residence time of 504 s.

The following figure 7 depicts the simulated particle path in the chamber as a result of the input-output configuration most of the particles are concentrated within the center and particles the bounce against the output wall have an extended duration inside the chamber.

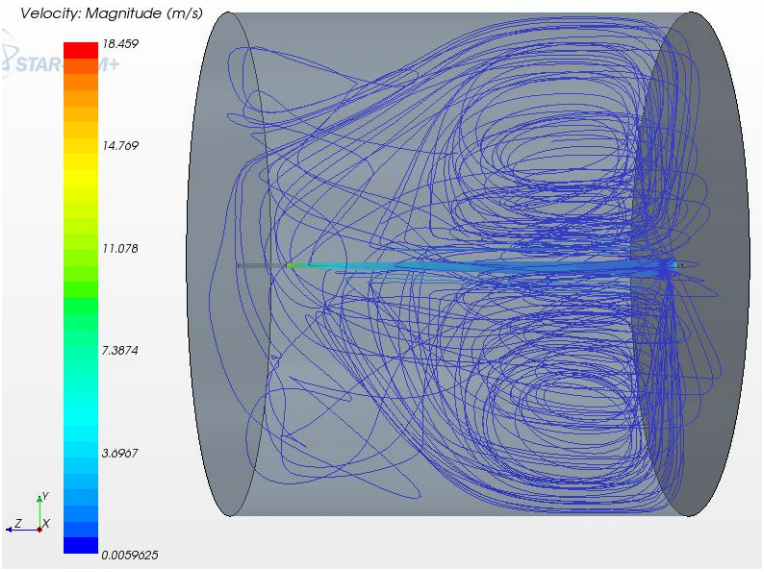

Figure 7. Streamlines inside the chamber.

The CFD simulation provided insight into the particle and gas distribution in the chamber while it is being filled and air is recirculated. The air residence of 504 s provides guidance on how long the chamber must be flushed between experiments to

avoid cross-experiment contamination and on the minimum filling time. In practice, however, these durations are determined based on measured particle concentration time series. The modeled streamlines assist in selecting the inlet and outlet configuration that provides the best mixing. Based on the results of the simulation, injected particles will be not homogenously mixed within the volume without forcing turbulence, as was done with the first generation chambers.

2.5 Particle growth rate

Particle growth rate is measured with a scanning mobility particle sizer (SMPS). The growth rate of particles in the chambers is analyzed through a sequence of size distribution measurements and used to determine the characteristics for the processing mechanisms. The growth rate will be the result of coagulation, gas condensation, and aerosol activation during cloud cycles. Low particle concentrations are desired to minimize the influence of coagulation,. For experiments for which higher particle concentrations are required, the growth rate measurements must be corrected for the contribution of coagulation. This procedure is easily applied and made more accurate by using narrow particle size distributions that can be easily tracked throughout the experiment. Accurate measurement of the growth rate requires minimization of any interactions of the particles with the sample tubing and any evaporation or growth resulting from temperature perturbations between the chambers and sampling instrumentation.

For experiments without aqueous phase chemistry, the mass transfer that is responsible for increasing or decreasing the particle size *Rp* is driven by the gas concentration gradient

$$R_p^2 = R_{p0}^2 + \frac{2D_g M_A}{\rho_p}(c_\infty - c_s)t \qquad (1)$$

Where c_∞ is the concentration far away from the particle, c_s is the concentration at the particle surface, D_g the gas diffusivity in air, M_A the molecular weight, ρ_p the particle density, and R_{p0} the initial size (Seinfeld and Pandis, 1998).

In the limiting case of growth due only to gas condensation, estimates of growth rate can be based on superposition of prior experiments for which only one precursor gas was added..

The growth rate resulting from aqueous phase chemistry is more complicated and involves a greater variety of reactions. To assess this growth a water vapor supersaturation is established in the chamber, resulting in activation of the seed aerosols to form cloud droplets, followed by interaction with soluble gases that collide with and diffuse into the drop. Interactions at the surface and inside the droplet include hydrolysis and/or ionization, aqueous phase diffusion off the ionic and nonionic species, and irreversible chemical reactions.

Individual tests on the growth rate following injection of different gases for experiments having very similar generated seed aerosols and test conditions will provide a foundation for interpretation of the growth rate when more complex gas mixtures are present. Subsequently, comparisons can be made between predictions based on those

single component experiments and experiments conducted with ambient air in which multiple compounds are condensing on dry and wet particles.

2.6 The 2nd generation chambers

The 2nd Generation chamber design relied on the successes achieved and challenges encountered with the 1st generation chambers, while also incorporating several significant modifications and improvements. Several key design parameters were established at the beginning of the design process and retained throughout the iterative and dynamic process from design to construction.

The main three elements of the chambers are:

1. Transparent to natural solar radiation to drive photo-oxidation processes.
2. Rotation of the chambers to minimize gravitation losses of larger particles.
3. Withstanding vacuum required to reach water vapor saturation for during experiments in which expansion is used to form clouds.

Each reaction chamber is made out of a single piece of heat-sealed FEP that transmits incoming natural solar radiation. The volume it encloses is linked to sampling and injection instrumentation through ports through FEP-coated end caps to which the FEP is sealed. Additional design criteria include reducing contamination sources and reactive surfaces by using Teflon components and coatings where appropriate, mimicking ambient conditions by using porous e-PTFE membranes, reducing thermal mass to facilitate the cloud cycle experiments, and use of tubing and connections in the

flow lines that result in low pressure drop. Supporting the chambers are additional modules for flow control, aerosol generation, and gas conditioning that were also design and constructed. The sampling equipment for measurement of size distributions, hygroscopicity, and growth rate were already available in our research group.

3. INSTRUMENT DESCRIPTION

The Captive Aerosol Growth and Evolution chamber system is distributed between two trailers. In contrast with most chamber facilities, this system had to be field deployable because the baseline gas composition in the chambers mimics ambient air, the characteristics of which vary significantly in different regions. This section describes the CAGE components and techniques developed, beginning from the instrument schematics and draft design and continuing through the final assembly.

3.1 Instrument layout

The amount and physical dimensions of the equipment interfaced with the chambers required the use of two separate trailers; one is a 30’ long flatbed trailer with the chambers and the other is a 20’ long instrumentation trailer 20’ that houses the additional modules and sampling equipment and has spare room for additional instrumentation during collaborative projects. An area of approximately 10 x 10 m is needed for the two trailers when positioned side-by-side. Attached to the flatbed trailer is the steel frame that supports both chambers, the stainless steel and Teflon lines connected to them, the chamber rotation motor and axles, the cabinet housing the flow control components, and the temperature control system. The instrumentation trailer houses the aerosol generation and gas conditioning systems, vacuum pumps, and sampling instrumentation. The instrument configuration is shown in Figure 8.

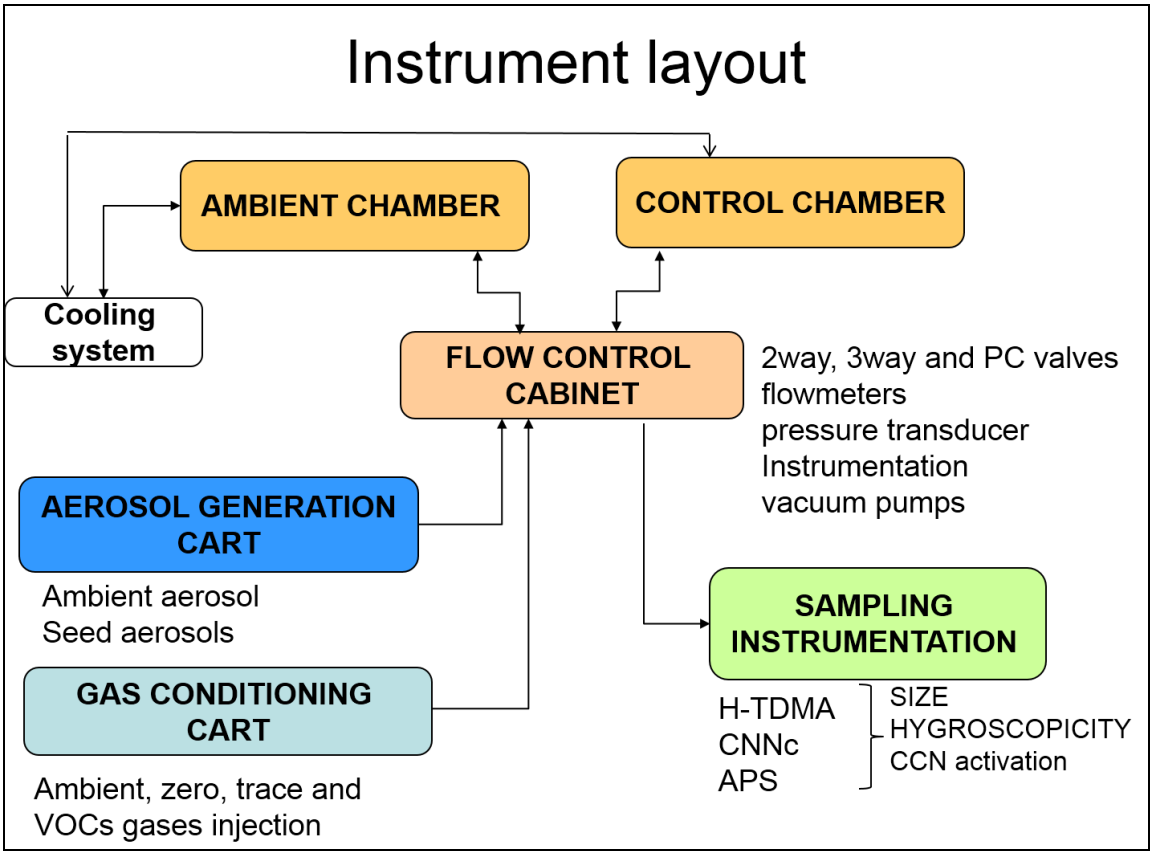

Figure 8. Elements of the CAGE system.

3.2 Chambers and integrated hardware

Many of the experiments for which the chambers were designed involve assessment of the response to slight perturbations in gas or particle chemistry. An example of such an experiment involves filling both with ambient air and the same type and size of seed aerosols, but adding to one chamber a trace gas such as NOx. By using this methodology, isolation and quantification of important chemical and physical

processes is simplified. This design specification required construction of a pair of identical chambers that would be operated simultaneously during an experiment. Both chambers share common lines for injection and sampling.

The chambers' supporting frame is a welded steel rectangular skeleton onto which the chambers, ducts, flow control cabinet, and chamber rotation motor are permanently mounted as can be seen in figures 9 and 10.

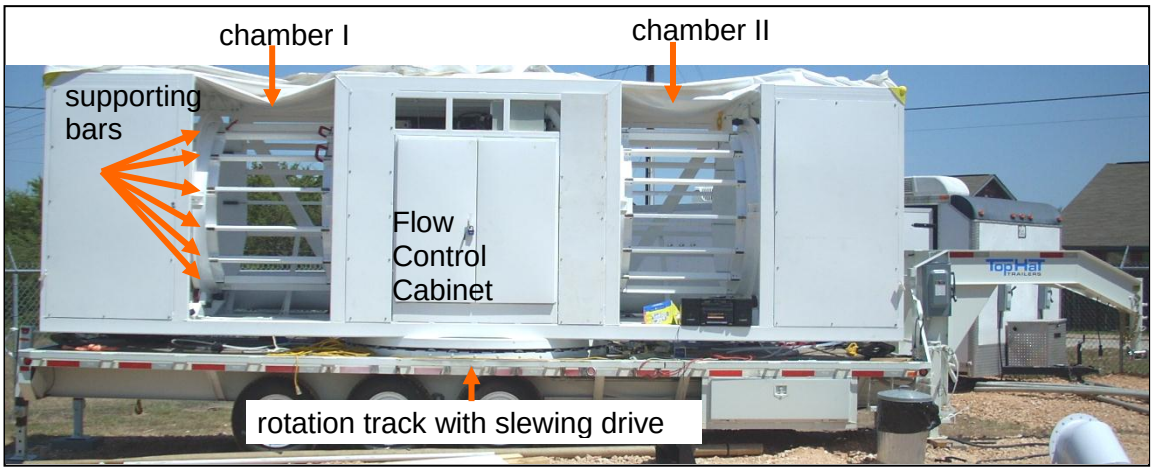

Figure 9. Flat-bed trailer front view.

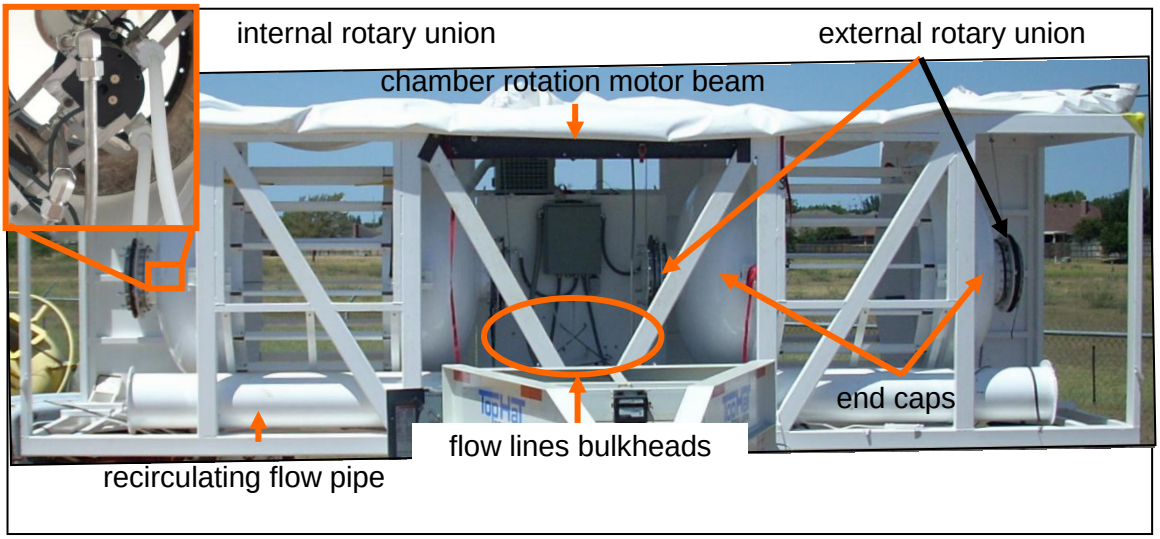

Figure 10. Flat-bed trailer back side view.

Injections into the chambers are routed through the outside end caps while particles are extracted through the inside end caps. Connected to the end caps are the external rotary unions, through which heated or cooled air flows to control the chamber temperature. The top of the frame is removable while the sides are attached metal sheets.

3.2.1 Chamber frame rotation

In an effort to maximize incoming natural solar radiation that is essential to drive photo-oxidation reactions, the frame supporting the chambers rotates on a vertical axis such that it is always perpendicular to the sun. This was necessary to avoid shadowing

from the frame and chamber end caps. The entire frame holding the chambers and part of the flow and pressure control systems (housed in the cabinet) are coupled to the trailer by two circular tracks. The trailer track contains (48) 4" diameter wheels and the frame track sits on these wheels. A slewing drive in the center intermittently rotates the frame orientation according to calculated time-dependent solar angle. A complete 180^{o} rotation requires around 10 minutes. An analog voltage-output rotation sensor attached to the middle section of the slewing drive provides a signal indicating the orientation.

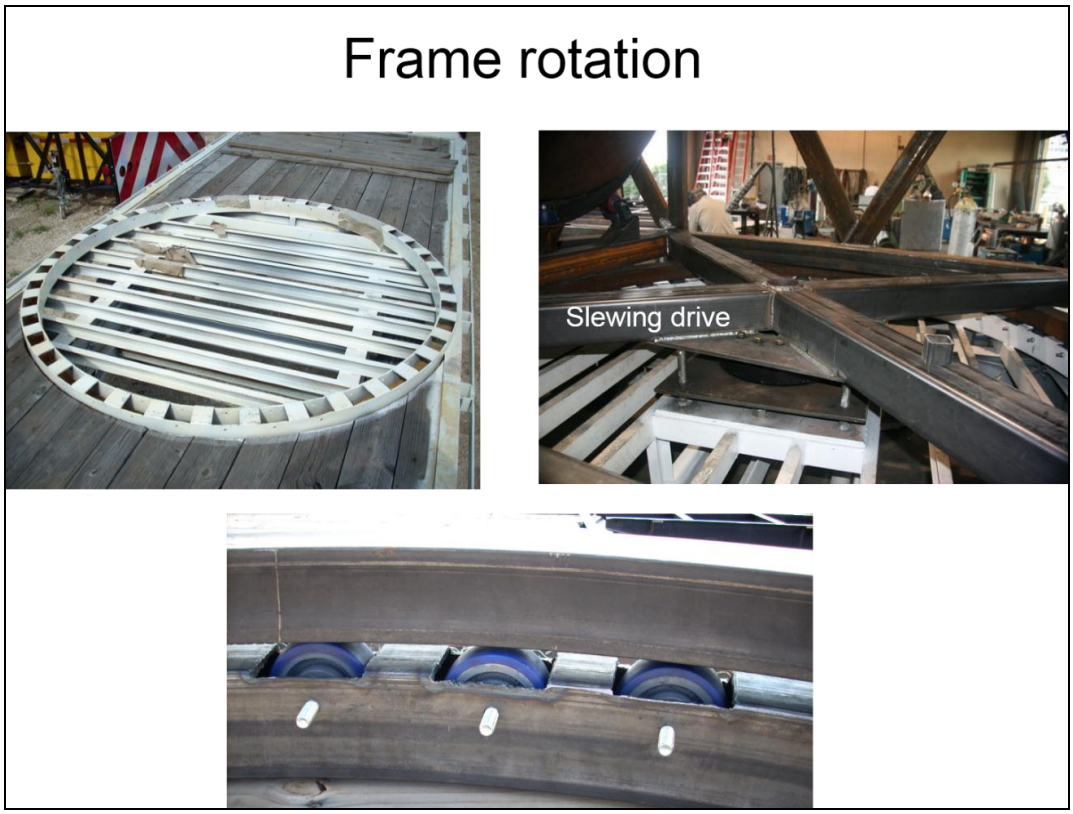

Figure 11. System used for frame rotation

Figure 11 shows the caster wheels used to support the frame and provide a fairly free rotation.

The steel frame directly attached to the slewing (figure 11, left top) drive has several openings for the power and signal wiring and the stainless steel, Teflon, and nylon tubing. Several electrical conduit pipes attached to the frame route the wiring and tubing towards the front of the trailer for connection to the instrumentation trailer.

3.3 Captive aerosol chamber

Elements of the design and some operational characteristics of the Captive Aerosol Growth and Evolution (CAGE) chambers are shown in figure 12. The major components of the CAGE chambers identified in the figure are described in detailed in the following sections.

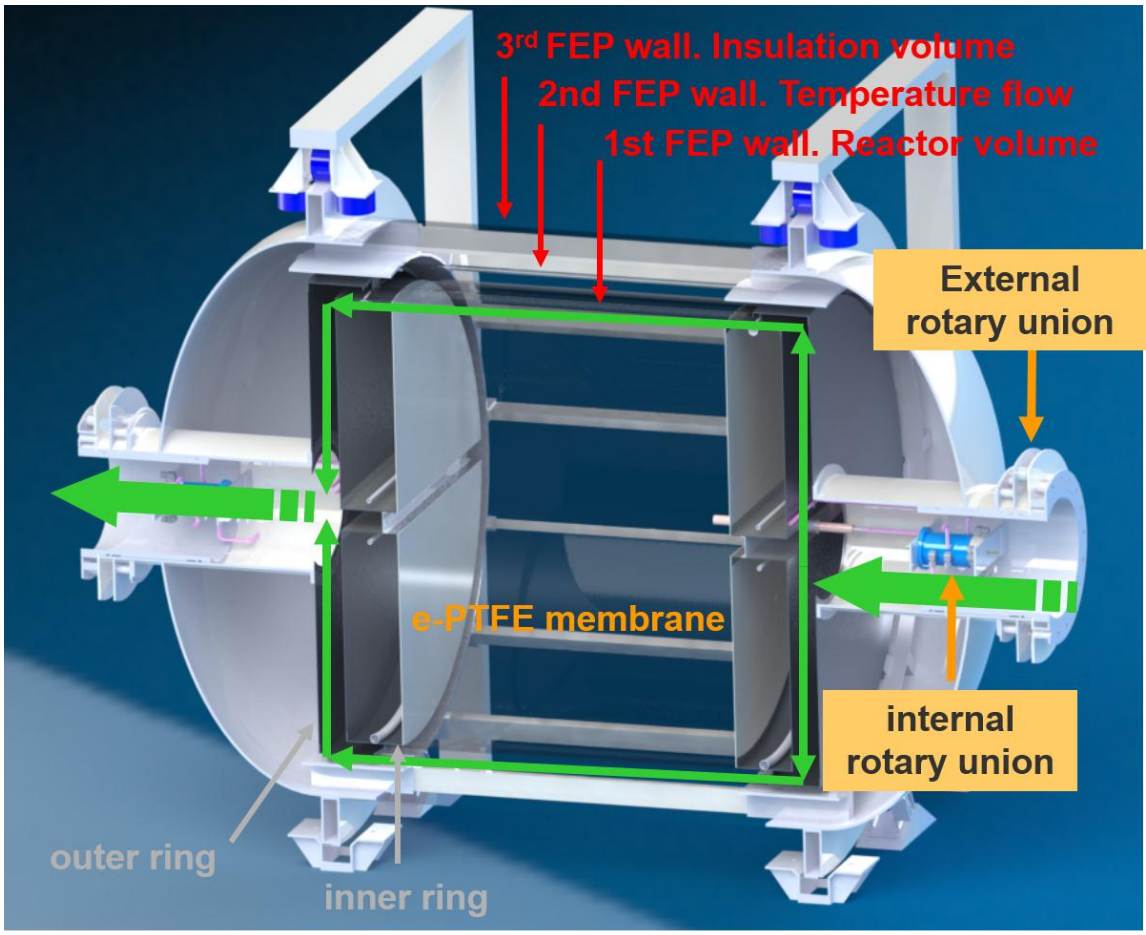

Figure 12. CAGE major parts

3.3.1 Chamber end caps

Following commercial vacuum vessel design, a cylindrical shape with hemispheric dome end caps was chosen for the outermost containment structure. Overall, there are a total of three end caps per side, with the internal two not required to

withstand the substantial pressure differential experienced by the outermost ones. The two outer caps are separated by 70 inches and held together by rectangular solid steel bars that minimally shadow reactor chamber. The resulting outer structure resembles a cage. The pressure exerted on the end caps and supporting bars was simulated using SolidWorks 3D Cad software. After several design permutations, a decision was made to use 15 equally-spaced bars that are 42 inches long, 3 inches wide, and 1.5 inches tall. This outer structure provides the needed strength to withstand the anticipated vacuum, but the enclosure it creates is not suitable for the reactor volume and, instead, additional concentric volumes that are described below were required.

3.3.2 Chamber rotation

Rotation of the chambers along a horizontal axis is achieved using a hollow shaft motor installed between the chambers and across a beam on the upper back side. Several components were welded to the end caps to transmit the motor rotation to the chambers. A rectangular tube bent to a diameter of 60” was welded to the cylindrical portion of the outer end caps at 5” from the edge. This raised ring rest on two spring-loaded wheels whose supports are welded to the floor of the frame. Four additional wheel structure supports holding three free rotating caster wheels are welded to the sides and top of the frame to restrain the chambers both during operation and transport.

In figure 13 the rotation parts are shown. A chain joins a sprocket welded to each end cap to a gear inserted in the main rotating shaft. The resulting rotational speed

is fixed to either 1.0 or 1.4 revolutions per minute by using different gears. If desired, the range could be increased by using a variable speed drive controller for the motor. Either chamber can be disengaged from the rotating shaft .

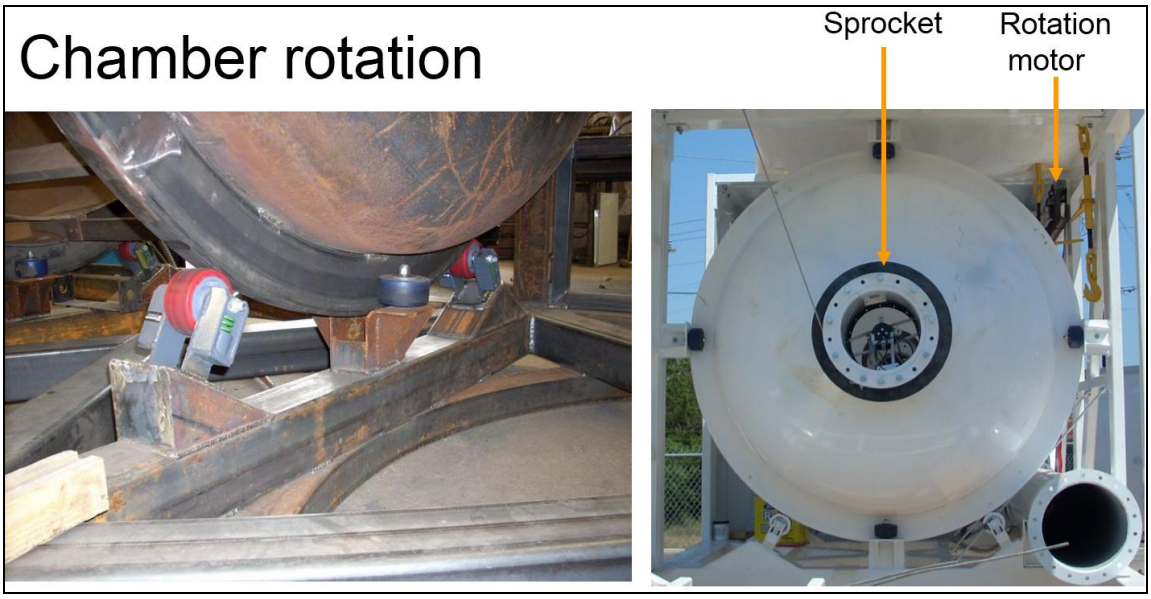

Figure 13. Spring loaded wheels and end cap support structure.

3.3.3 Reactor chamber volumes

The chamber internal volumes are bounded by three concentric FEP transparent sheets, each of which is sealed at both ends. Figure 14 shows a cross section of the 3D

model designed in SolidWorks showing a single chamber sitting on its supporting frame.

The design and function of the chamber volumes are detailed below.

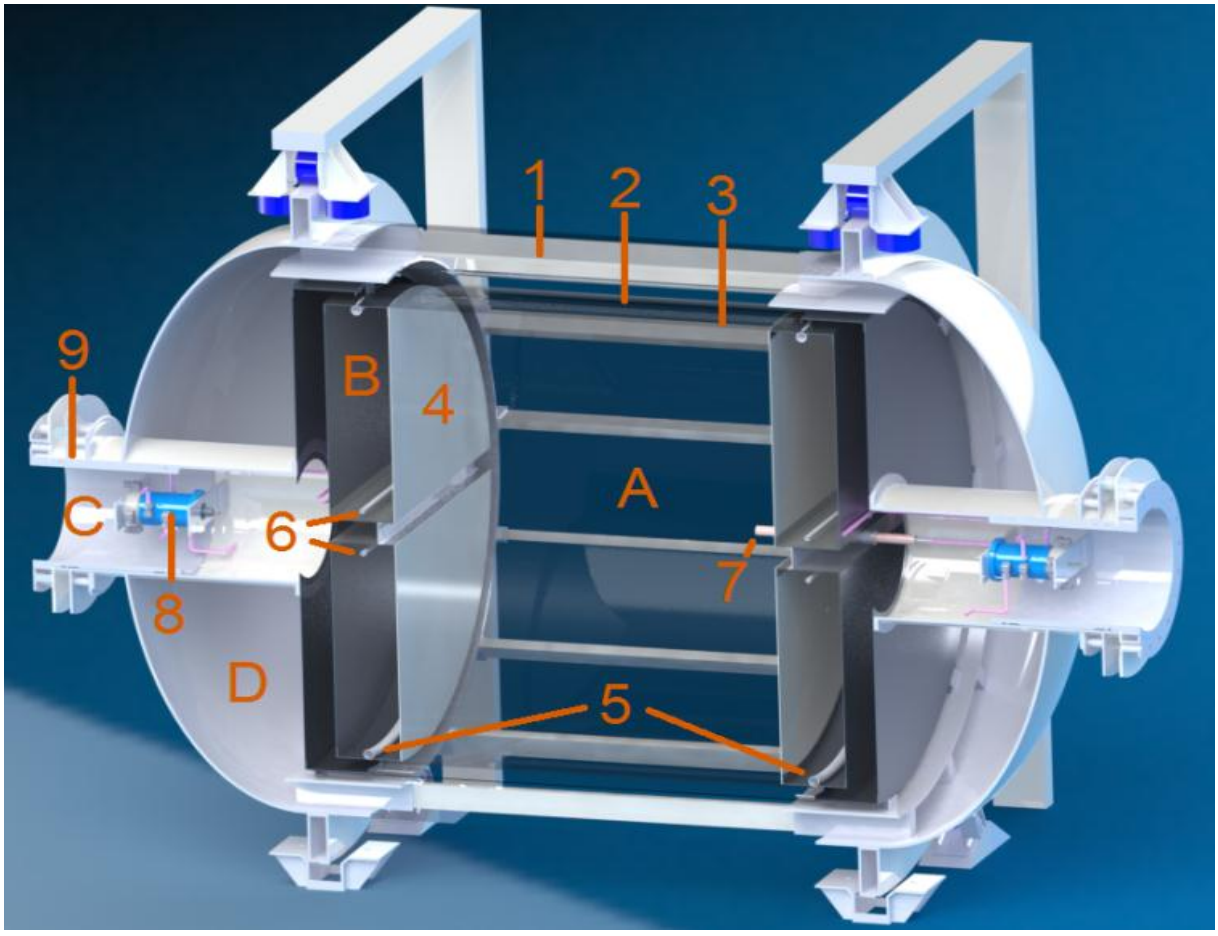

Figure 14. Chamber components. A) Reactor volume; B) Gas exchange volume; C) Recirculating temperature conditioning Flow; D) Stagnant Insulating Volume ; 1) Outer FEP layer, 5 mil; 2) Middle FEP layer, 3 mil; 3) Inner FEP layer, 3 mil; 4) ePTFE gas exchange membrane; 5) Gas exchange Teflon lines, perforated extraction line; 6) Gas exchange line, perforated extraction line; 7) Aerosol sample injection port (similar extraction port not shown on opposite end); 8) Internal rotary union; 9) External rotary union.

3.3.4 Insulation volume

The outer layer of 2 mil thick FEP film (Figure 14 - 1) encloses a thin layer of stagnant air that serves as an insulating volume (Figure 14 - D). This is also the layer in which the minimum pressure is found. The ends of this volume are within the metal hemispheric end caps.

Just towards the chamber side of the rotation track ring described above, a cylinder was welded to the end cap to provide the surface onto which the outer FEP cylinder is sealed. The temperature conditioning air that circulates around the chambers is introduced through the external rotary unions that were connected through holes cut into the centers of the end caps (Figure 14 - 9). Specifically, a specially machined 14" diameter pipe extending 24" to the inside and 16" to the outside was welded through each end cap. Into this slides a tight-fitting mating pipe that connects to the air conditioning system located immediately behind each chamber. This inner pipe remains stationary while the end cap and chambers rotate. Considerable design and machining effort was required to achieve the necessary tolerances to achieve a seal along the o-rings separating the inner and outer pipes.

The high strength steel bars surrounding the chambers that are described above were wrapped with highly reflective ePTFE gasket and covered with heat shrink transparent FEP. In figure 14, seven of these bars are visible. A plastic coated steel wire wraps around the rectangular solid bars with about 4" gap between each turn to provide an additional support surface for the outer FEP cylinder while it deflects under vacuum.

3.3.5 Temperature control volume

The middle air layer (Figure 14 – 2) separating the insulating layer from the reactor volume is used for temperature control. A high flow inline blower recirculates air through a cooling coil and resistive heating elements and then through the temperature control layer in each chamber. The cooling liquid pumped through the cooling coil and the current passed through the electric heaters are adjusted to control the temperature of the air to track either ambient temperature or the temperature inside the reactor volume during cloud formation. The active temperature control approach also reduces thermal gradients during all experiments that would otherwise increase turbulence and, consequently, particle loss rate. The pressure in this layer is maintained slightly above that in the insulating layer to keep the FEP cylinder inflated and sufficiently taught to minimize movement that would induce turbulence and mixing inside the chamber. The volume is contained between two thin aluminum rings at the ends and the FEP cylinder along the sides. The aluminum rings are 51” in diameter, and 0.125” thick and are attached to the outer steel end cap by 7 tabs. The temperature controlled air passes through a 14” diameter hole that matches the diameter of the rotary union pipe through which it first enters the chambers. Mating welded flanges seal the aluminum ring to the rotary union pipe. The middle FEP cylinder slides over these rings and is secured by Teflon-coated wire that is tightened using turn buckles.

3.3.6 Reactor volume

The reactor chamber volume defined as a minimum of $1m^3$ basically outlined the remaining pieces dimension. An upper limiting size was the result of the need to be deployable, while a smaller size was desired for a fast gas diffusion speed through the ePTFE membranes into the volume and a reduced exerted pressure while holding vacuum.

The inner layer of FEP film (Figure 10 – 3) 2 mil thick is the reactor volume (Figure 10 - A). It is made of an FEP bag 3 mm. thick and two supporting inner aluminum rings with 48" diameter with welded tabs on the outside. It is attached to the outer aluminum ring. The FEP bag slides over these rings and is secured in place by a Teflon coated wire adjusted by turn buckles. Inside the outer rotary union there is a small rotary union (Figure 10 – 8) with four 3/8" FNPT ports and slipping rings for signal wiring. The flow connection to the reactor and insulating volumes are done via the internal rotary union.

3.3.7 Eptfe membrane

The inner ring has two lobes covered with ePTFE membrane (Figure 10 – 4) for the gas exchange between the chamber and the gas conditioning flow. A set of snubs welded between the lobes vertical walls are connected to half inch O.D. FEP perforated Teflon tubing that distributes the gas conditioned flow. Flow is directed from the far

inner edge towards the middle section. Figure 15 shows the two lobes that are divided by a 3" wide central rib used to provide rigidity and support for bulkhead connectors. The lines coming out from the chambers flow through the inner rotary union.

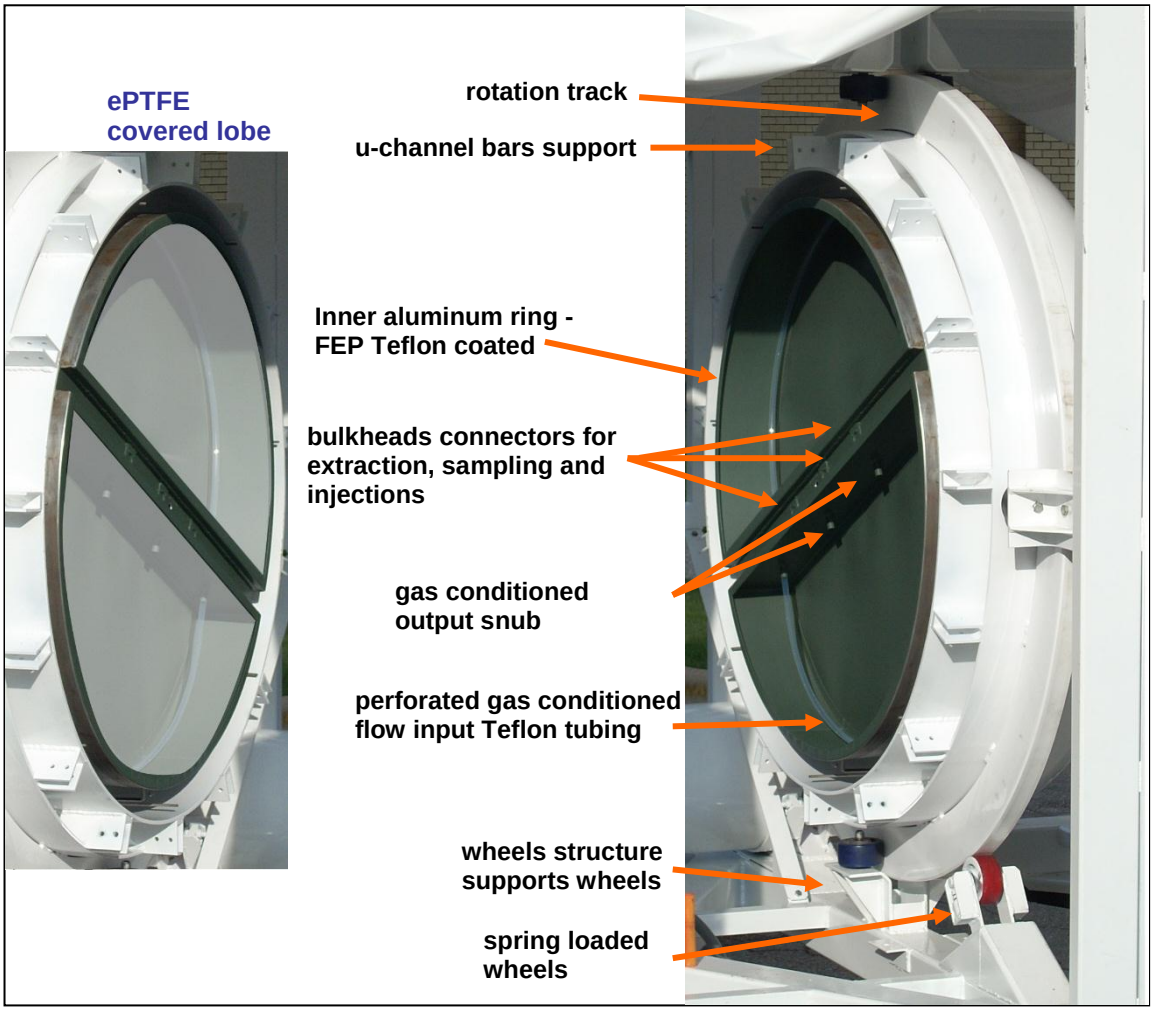

Figure 15. Inner ring inside the end caps.

The diffusion scales from behind the ePTFE membrane into the reactor volume were measured in the 1st generation chambers and have to be measures for this instrument. In order to reduce the diffusion scale this design has two ePTFE membranes.

3.3.8 Differential pressure

The flow rate is controlled by proportional control valves and critical orifices. The critical orifices fix the maximum flow rate and the proportional controlled valves adjust it. For the most critical part, which is the two inner FEP bag layers instead of relying on electronic feedback control loop, there is a set of adjustable valves with a fixed pressure drop (indicated by $\Delta P \alpha V(\varnothing)$). This way, the small differentials pressures are kept fairly constant during experiments and also assure repeatability as long as the same flow rate is used. The differential pressure implies the most critical operational step for the systems, and consequently, a failure would probably rip the FEP bags. Figure 16 show the desired pressure between the different chamber volumes that would provide the best working condition.

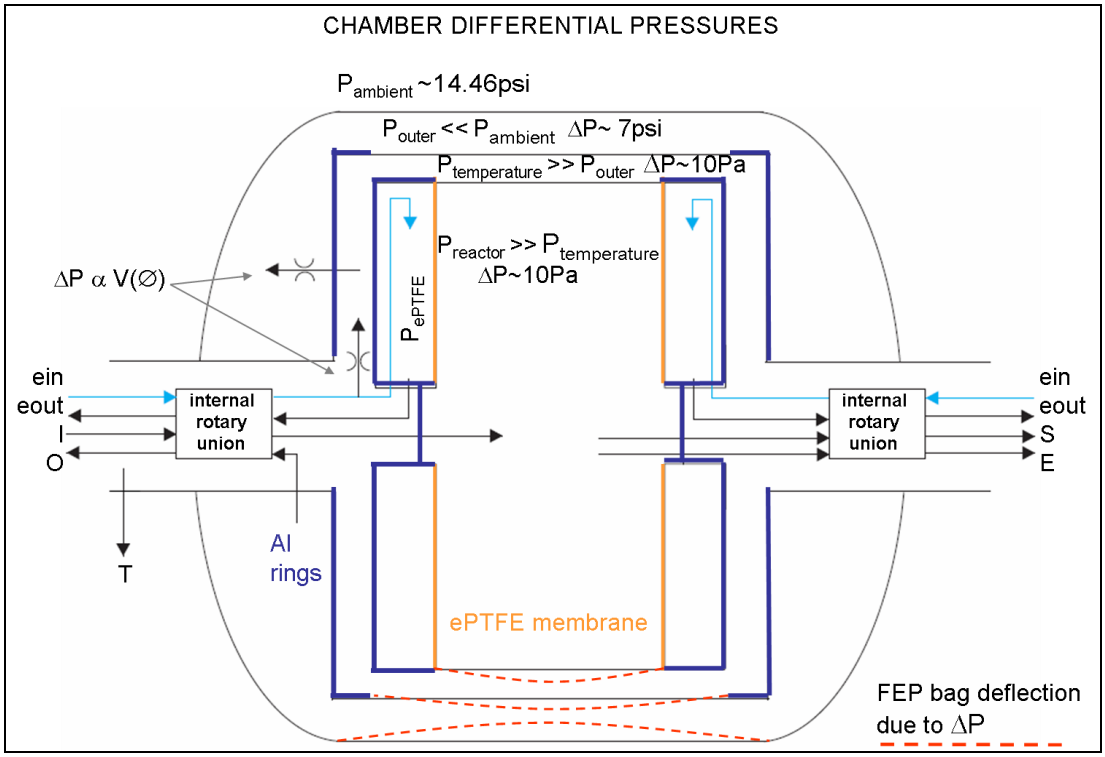

Figure 16. Concentric volumes differential pressure.

The differential pressures have the effect of making the bags taut, thus reducing the induced turbulence caused by the temperature controlled high flow rate. The process of inflating and deflating the bag will most likely create wrinkles the effects of which will be monitored throughout experiments. In the same way, the reactor volume outlines the equipment dimension, and the reactor inner pressure determines the pressure drop required for cloud formation, this pressure being always below ambient pressure.

Pressure drop is given by flow speed and routing components composed of ePTFE membrane, connectors into the internal rotary union, rotary union, tubing

between the chambers and cabinet, valves inside the cabinet, tubing to the aerosol cart, gas conditioning cart parts, and finally, a Teflon filter located on top the instrumentation trailer.

3.3.9 Flow lines

The flows lines are used for injection and sampling of aerosols and gases and also for the injection and extraction of gas conditioning flow. There is a line for vacuum. Both inlet and sampling line, located in the center of the aluminum rings extrude 8 inches towards the inside. A retractable system is to be implemented allowing the injection and sampling at different positions up to the middle of the chamber along the center axis independently. Several stainless steel and Teflon tubing lines, communication and electrical wiring are run on the side of the trailer towards the front for their connection to the instrumentation trailer.

3.4 Auxiliary modules

There are three modules with distinct functionalities connected to the chambers. On the mainframe is the flow control cabinet, while inside the instrumentation trailer are to be found the aerosol generation cart and the gas conditioning cart.

3.5 Flow control cabinet

The Flow Control Cabinet (FCC) is a central module for flow routing and control. It interconnects the chambers to the aerosol cart, the gas conditioning cart and sampling system. The cabinet is located between the chambers on the front side of the main frame.

The back side of the cabinets has 3/8” and ½” bulkhead connectors, ½” grommet protected holes and electrical bulkhead connectors. The three vacuum pumps identified as V1, V2 and V3 are located outside the cabinet into the instrumentation trailer.

The FCC is welded to the frame and to work on the FCC the entire systems is rotated 90 degrees that way a person can stand on the flatbed trailer to make modifications. There is space available on the right upper corner to place an instrument that is connected to the sampling line. In the following figure the instrument can fit either CPC or APS instrument. The rest of the instruments can be located in the instrumentation trailer which has available space and power lines. The FCC has two doors that fully open providing easy of access to work on it.

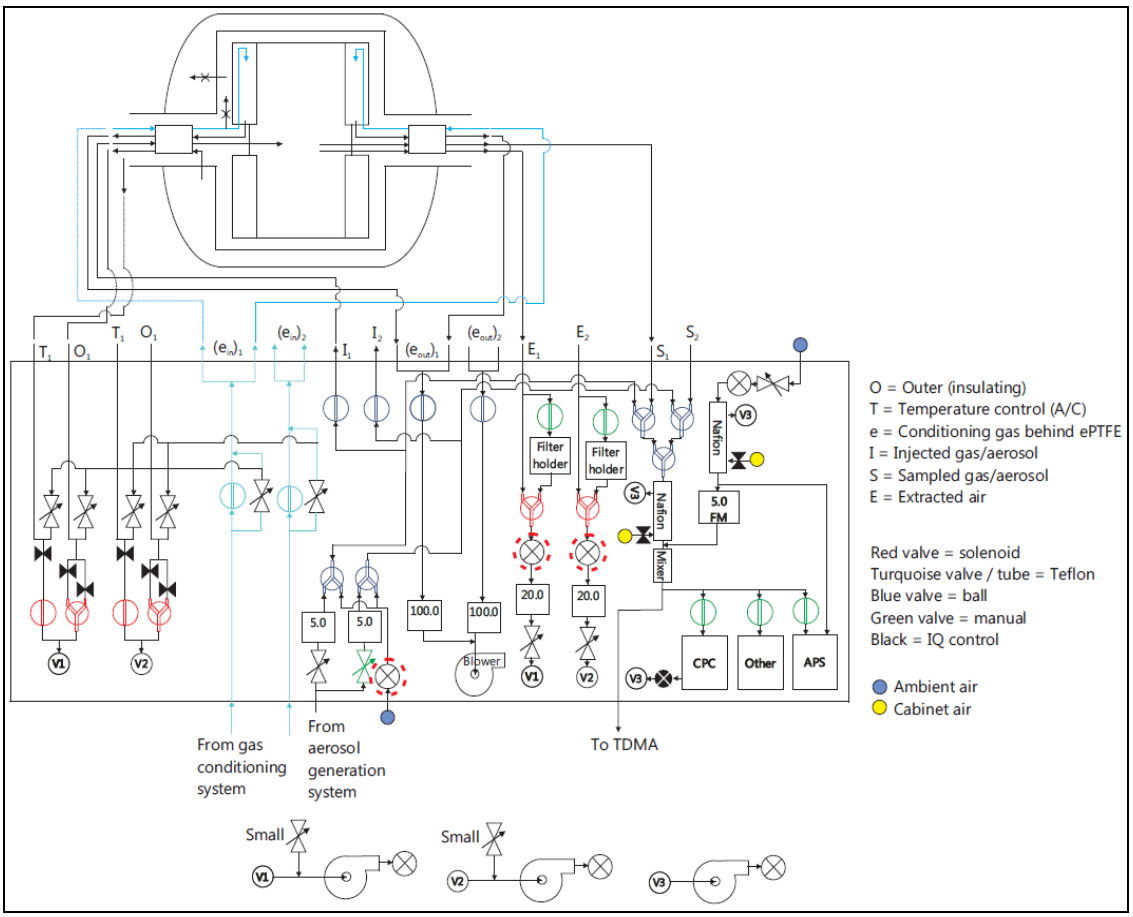

Figure 17. Flow control cabinet schematic

Figure 17 shows that the reactor volume is connected to the tubing lines identified as injection line **I**, sampling line **S** and extraction air line **E**.

-The gas conditioning flow behind ePTFE is connected to line $\mathbf{e_{out}}$ and $\mathbf{e_{in}}$.

-The recirculating volume is connected to vacuum pump via the **T** line.

-The insulation volume is connected to vacuum pump via the **O** line.

Flow from the Aerosol Generation Cart containing the seed aerosol and gas runs to the injection or I_{flow} 3/8" stainless steel line. The flow is split into two lines. The first one goes through a proportional control vale into a 5LPM Allicat Flow meter and to the normally open port of a 2way pneumatic valve. The second one moves towards a manual valve into a 5LPM Allicat Flow meter and to the normally open port of a 2way pneumatic valve. The normally close port of both 2way valves is connected an open air inlet on the top of the cabinet to inject ambient particles into the chambers and characterization. The aerosol injection line is directed to the chambers (bulkhead labeled I1 or I2) or the sampling line. The common port of the 2way pneumatic valves goes to a tee splitting the flow towards the chamber, going through a normally closed one way pneumatic valve, or to the sample lines downstream of the chamber allowing the injected flow to be characterized by the instrumentation.

The sampled gas / aerosol are the S_{flow} stainless steel 3/8" line. A set of three 2way pneumatic valves allows sampling from the I_{flow} or S_{flow} of the chamber. The common port of the chamber selective 2way pneumatic valve is connected to a Nafion drier and a mixer to dilute the sample if required. The dilution is used to slow down the particle concentration decrease while sampling for long duration experiments. The line is driven by the vacuum pumps used on the instrumentation. The output is connected to instrumentation housed inside the cabinet and a line that connects to the instrumentation trailer, where the TDMA and other instrumentation are located.

From the chambers the E_{flow} (extracted air) stainless steel 3/8" line has a tee to direct flow to the normally open port of a two way valve or towards a filter holder which

is connected to the normally closed port. The common port is connected to a 20LPM Allicat flow meter, a proportional control valve and to the vacuum line. This line is used to collect particles into any type of filters (metal housing filter, bubbling system, etc). It is also used to purge the chamber at high flow rate after experiments.

Flow from the gas conditioning cart e_{in} and e_{out} lines (¾" Teflon) are connected to a Teflon valve and proportional control valve and these are connected to the inner aluminum ring lobes feeding the area behind the e-PTFE. The e-PTFE gas is pulled by a blower located in the cabinet. This flow goes through a one way pneumatic valve and a 300 LPM TSI hot wire flow meter. The outputs of the flow meter are tied together via software connected to the inlet of the Ametek Windjammer blower. Flow is controlled using PID feedback loop. The two 3/4" lines from the aerosol cart feed through the slewing drive into the cabinet holes labeled e_{in} and e_{out}.

The pressure control of the chamber layers are connected to the O_{flow} lines , namely the Outer (insulating) layer and the T_{flow} or temperature control line. For the aerosol flow path, pneumatic valves are used. These valves do not use oil for lubrication reducing possible contamination sources into the flows. The valve configuration of either normally open or close was chosen for each valve according to its position to be used as safety paths in case of power or compressed air disruption.

The equipment housed inside the FCC is shown in the figure 18.

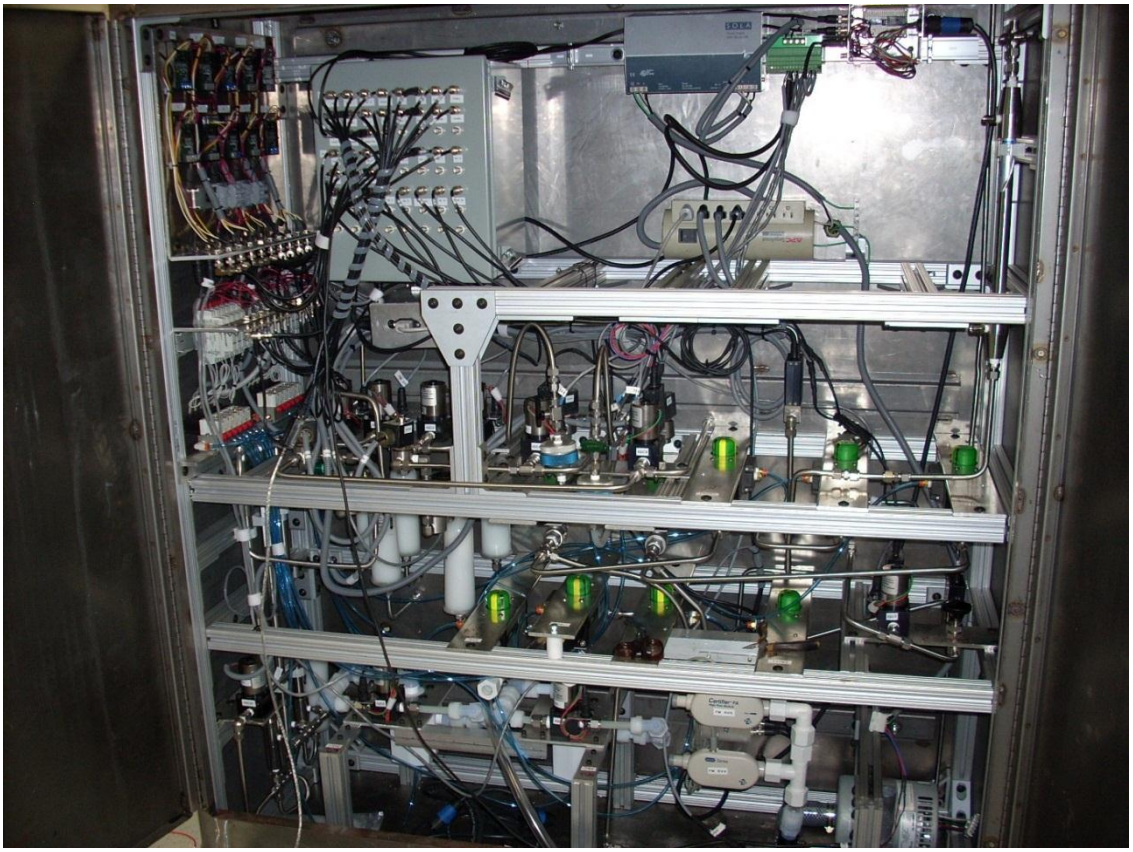

Figure 18. Flow control cabinet components

Behind the cabinet an outdoor electrical panel distributes the power coming from the front of the goose neck trailer manual switch breaker and has the solid state relays and protection to control the motor, blowers and temperature control equipment. The connectors are water proof and additional space within the conduits is available in case of the need to use more wires. The command lines and power lines are separated in order to reduce possible electrical induced interference.

3.6 Aerosol generation cart

The purpose of the Aerosol generation cart is to furnish seed aerosols to the chambers. The type of aerosols to inject for characterization purposes can be salts i.e. ammonium sulfate or polystyrene latex (PSL) monodisperse beads. It is connected to the FCC and gas conditioning cart. After a couple of field experiments of using atomizer for experiments a decision was made to assemble a unit with multiple configurations, better and stable performance output.

3.6.1 Description

The following figure 19 has the configuration design as of October 2012. The configuration was selected to be used in the field experiments that were performed at the Army Research Laboratory.

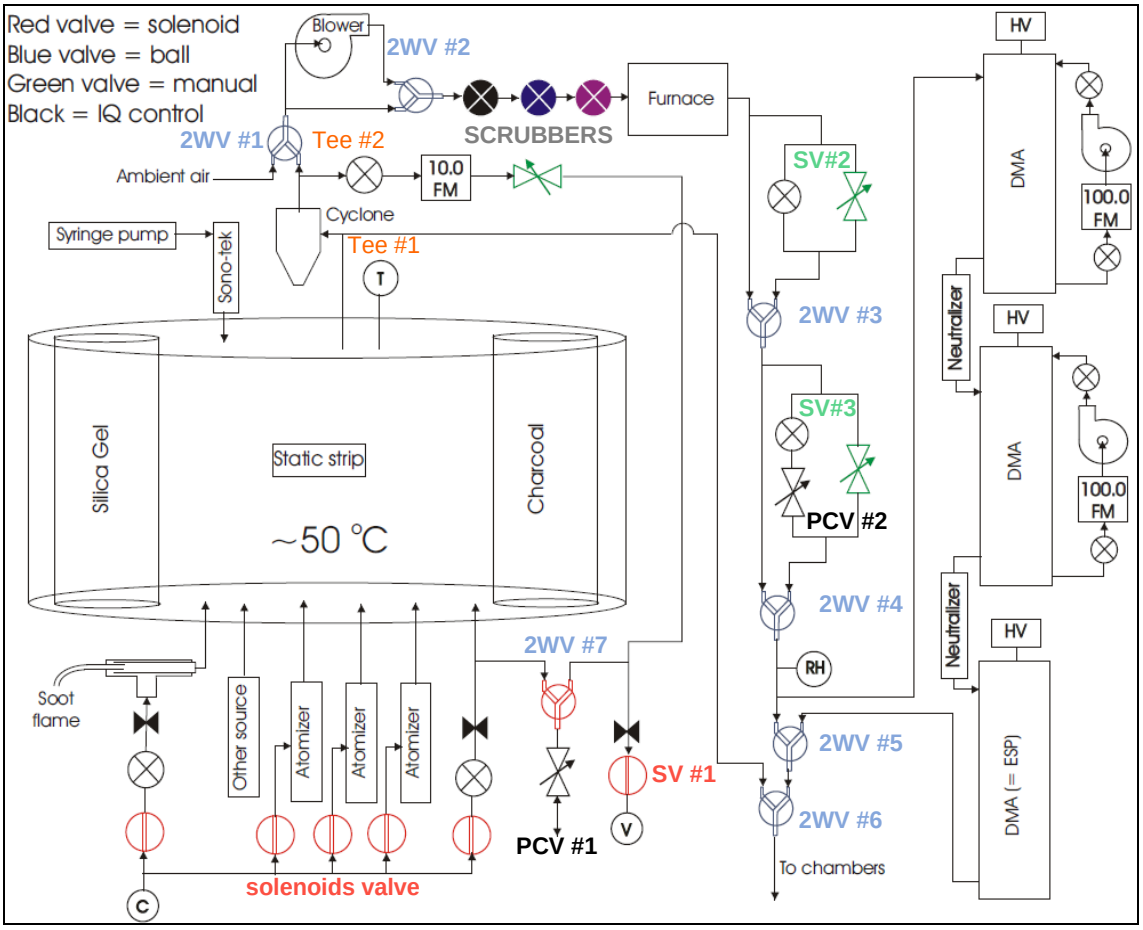

Figure 19. Aerosol cart generation system schematic.

The mixing volume is made out of stainless steel with multiple inlets allowing interchangeable configuration. The top and bottom plates have several FNPT ports. The default injection has three TSI 3076 Model Atomizers controlled by independent solenoid valves driven by filtered air compressed line at 30 psi. Additional injections ports allows for connection of soot generation and an ultrasonic nebulizer on the top. A

pair of canister with activated charcoal and silica gel inside the mixing volumes reduces aromatics and higher molecular weight organic and water vapor content. The mixing volume is kept constant at a temperature of approximately 50°C by a band heater.

A ^{210}Po (400 µCi) charging source brings the aerosol to neutral charge equilibrium state before exiting the mixing volume. The source is attached to a removable small cover lid with a feed through connector, supplying voltage for a small electric mixer fan.

The output of the mixing volume has a Tee #1 that will be connected to a cyclone (not installed by January 2012) with a cut off size of 1.5 µm while the other output is routed to the normally close port of a two way valve (2WV #6) whose output is the Aerosol cart output.

Upstream the cyclone, there is Tee #2 and a two way valve (2WV #1) selecting between the outputs of the cyclone –normally open port - or ambient air –normally close port-. The flow coming from this valve can be routed to a regenerative blower or directly into a scrubbing system via a two way valve (2WV #2) with silica gel, activated charcoal and mixture of permanganate and phosphoric acid coated charcoal running into a furnace. The furnace is intended to produce very fine aerosol as ammonium sulfate is vaporized and re nucleates. From there the particles flow directly into to the chambers or into an electrical mobility particle size classifier via a two way valve (2WV#5).

A recirculation path and critical orifices on the mixing volume adjust the output flow and dilution by means of two way valve (2WV#7) and a solenoid valve (SV #1) connected to a vacuum line. The path made of two way valves (2W#3 & 2W#4),

solenoid valves (SV #2 & SV #3), filters and proportional control valve (PCV #2) is used to adjust the flow rate.

The FCC can route the flow from this cart back into the instrumentation trailer for characterization of the seed aerosol before injection into the chambers.

3.6.2 Particle classifier

Particle coagulation is one the physical process reducing the aerosol concentration inside the chamber. As a poly disperse coagulation is more efficient than mono disperse coagulation, a higher particle concentration after experiments will be available by injection of a single mono disperse type size distribution.

Concerning experiments, seed aerosol will consist of a set of small and large monodisperse aerosol. The purpose is to have a better indication than change in overall aerosol mass or concentration of the amount of material condensed.

The particle size classifier narrows the poly disperse size distribution generated by the aerosol atomizer into a mono disperse size distribution using a high flow Differential Mobility Analyzer (DMA) with two columns in series, and finally, an electrostatic precipitator. Aerosols are first classified by the 1^{st} DMA column applying a fixed voltage, then routed into the 2^{nd} DMA columns with also fixed voltage but with a slight offset from the previous voltage, and finally, into the 3^{rd} DMA column. The last column is configured as an electrostatic precipitator with no sheath flow and a fixed

applied voltage of 5000 volts so that the aerosol output should be with zero charge. The output is a distribution of size-resolved aerosol.

Aerosols are neutralized between DMA columns to remove possible multiple charged particles. The additional 2nd DMA column is part of an integral redesign of a previously used injection system, narrowing the size distribution, and more importantly, reducing multiple charged particles which are lost at a faster rate than zero charged particles.

An additional feature from previous used DMA configuration is the high flow rate, capable of setting the sheath flow above 100 LPM. It is achieved by using two regenerative blowers in series allowing for faster injections time into the chambers than the previous design. The output is up to 10L/min mono disperse uncharged aerosols.

Teflon material is always negatively charged with an electric field voltages of -300 ± 150 volts/cm. Ions concentration can be measured by measuring the neutralization rate of single charged particles, and values range from 4 to 30 ions.cm-3. (McMurry and Rader, 1985)

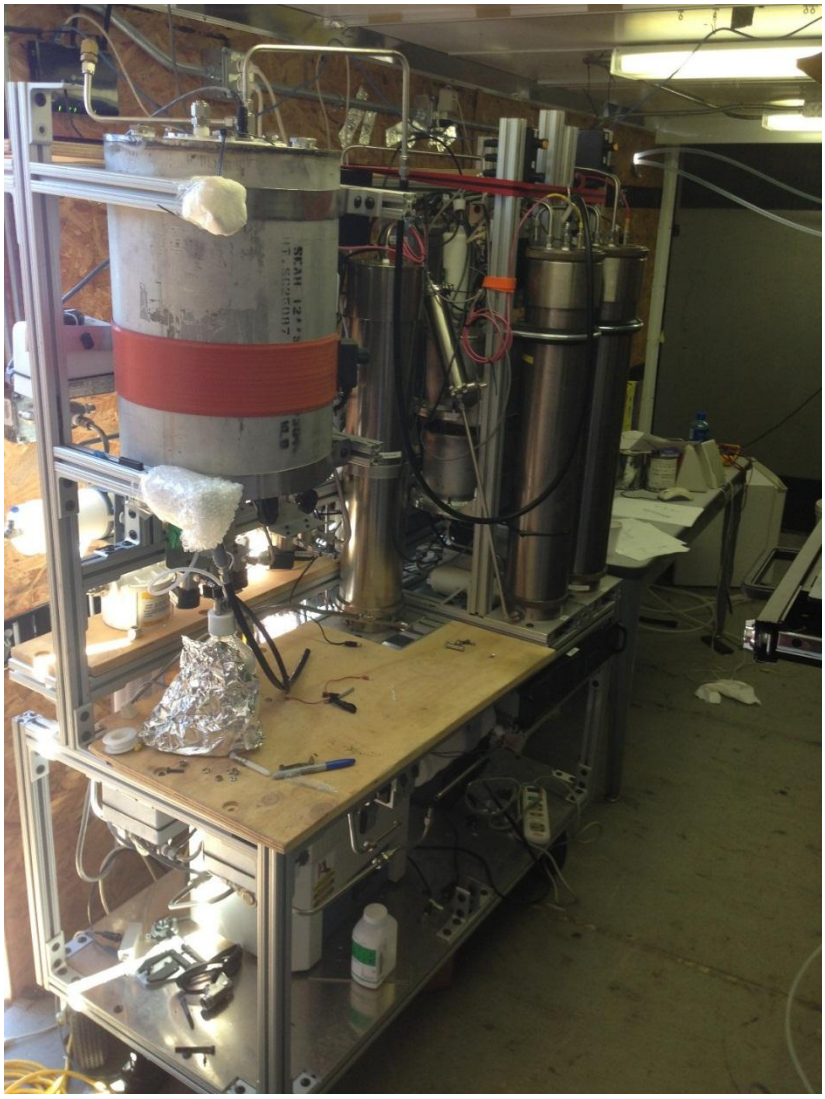

Figure 20. Aerosol generation cart inside the instrumentation trailer

Figure 20 shows the aerosol generation cart partially assembled. Below the aluminum cylinder with an orange band heater is available room for the seed aerosol.

3.7 Gas conditioning cart

The purpose of the gas conditioning cart is to provide the chamber gas Exchange sections of the reactor chamber with ambient air, filtered air, adjustable water vapor, high ozone concentration and a quantity of mass flow controlled VOCs.

3.7.1 Description

The following figure 21 has the configuration design as of October 2012. One of the reasons to assembly the gas conditioning cart is to have a stable system to produce very similar gas conditioning flow, experiment after experiment. The repeatability of this gas composition is required to make inter-experiment comparisons. Within the duration of field campaigns, 3 to 6 weeks, subtle changes for example in the scrubbing filter system can be expected which should not affect the measurements. The entire frame has four wheels moving it easily.

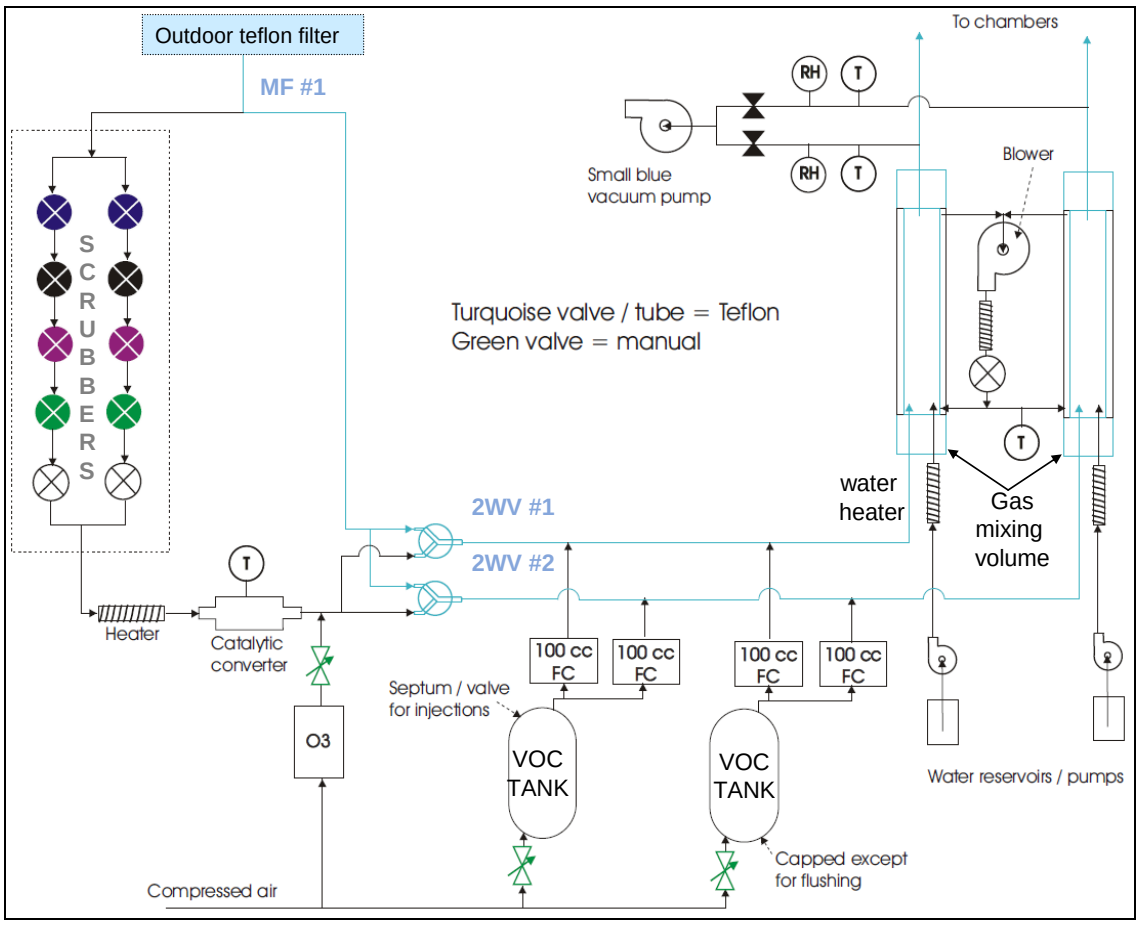

Figure 21. Gas conditioning cart schematic

The inlet to the system is a 1" Teflon line from the roof of the trailer connected to a Teflon coated filter supported on a Teflon frame. A Teflon custom machined manifold (MF #1) has a 1" FMNPT inlet and two ¾" FMNPT outlets. The inlet connects 1" tubing coming from the Teflon filter located outside the instrument trailer while the first outlet is connected to a pair of two way Teflon ½" valves (2WV #1 & 2WV #2) and the

second outlet is connected to a scrubbing system. The inlet flow can be split in two, and by using two independently controlled pneumatic valves, each chamber is run with either ambient air or zero air.

The scrubbing system modifies ambient gas composition into close to zero air, and it is composed of two banks with 4 canister filters from Parker which are 20" long and 4" in diameter with ¾" NPT stainless steel Swagelok connectors. The flow splits in two reducing pressure drop along the scrubbers. A stainless steel tube with perforated slits is attached between the bottom and top, and the air flows from the top in between the canister and the tube (scrubber material filled volume) entering through the slits towards the outlet port. The first filter is filled with silica gel, a combination of non-indicating and indicating type turning from blue to purple when it is ready to be regenerated. The second filter contains activated charcoal Spectrum XB-17 from General Carbon for the removal of organic compounds (toluene, isoprene, acetic acid, and nitrobenzene) and alcohols (isopropanol and methanol). The third filter contains Spectrum HS-600 from General Carbon, a silicate compound impregnated with 6% potassium permanganate ($KMnO_4$) for the removal of polar and lower molecular species. The fourth filter contains phosphoric coated activated charcoal for ammonia removal (Caffrey et al, 2001).

The scrubbing system was tested, figure 22, with a Gas Chromatography instrument from Dr. Gunnar Schade research group by the research assistant Johny Gramman. One ambient air and three filtered samples were run. From the test, the scrubbers reduced the baseline concentration by half and cut down most of the major gas

spikes. During field experiments analytical chemistry instrumentation should provide ambient gas composition to assess the oxidation pathways and the scrubbed gas composition.

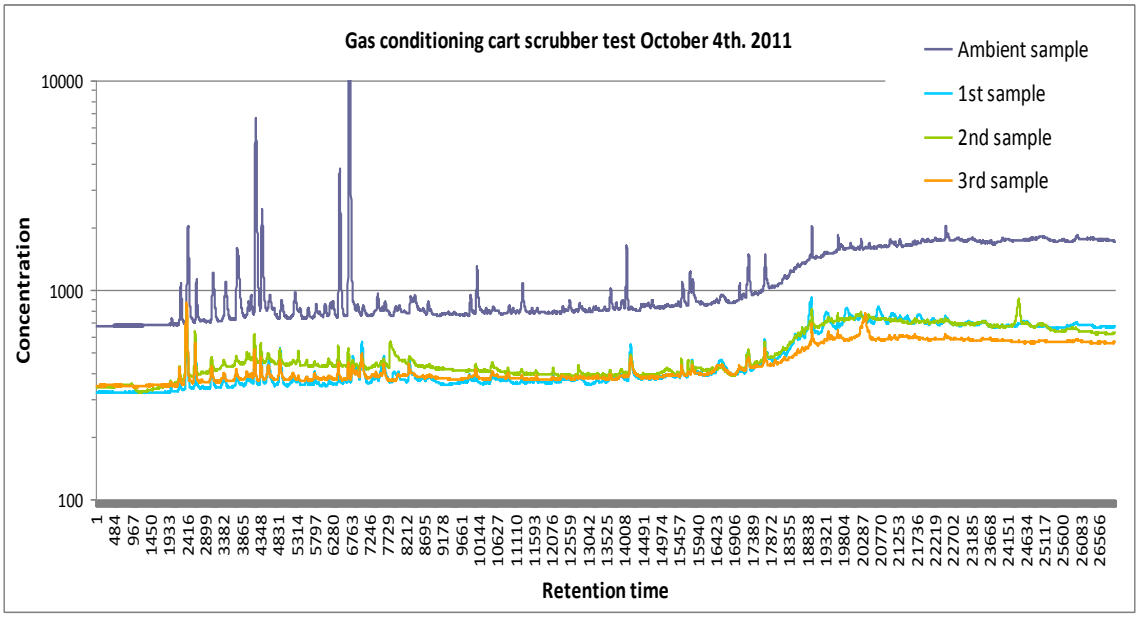

Figure 22. Scrubbing system gas chromatography measurement.

Before entering the Teflon two way valves, air from the scrubbers flows through a 1000Watt air heater into a catalytic converter and then to a force air helicoidally bent cooling tube. The common port of the Teflon valve is connected by ¾" tubing to the gas mixing volume.

3.7.2 Gas injection mixing volume

The gas injection mixing volume consists of 3” diameter FEP semi rigid heat shrinkable tube. It has four inlets and one outlet. The bottom cap is a custom machined Teflon manifold with 3 different sizes FNPT threads and a Teflon upper cap.

A wider outer transparent acrylic tube support the semi rigid FEP. The air between the FEP semi rigid tube and the acrylic support is recirculated passing through a heater reducing possible condensation on the walls. Air is filtered by an HEPA filter

The bottom manifold has a diameter of 3” with a main ¾” FNPT injection port for ambient or scrubbed air. Additionally there are two ¼” FNPT VOCs injections port connected to the mass flow controllers and a 1/8” FNPT water vapor injection port connected to a Yok-LOK stainless steel fitting.

The output port, located on the top, is a ¾” FNPT port with a reducing union tee. The main output is connected to the gas exchange chamber by a ¾” Teflon line and the reducing tee output is connected to a dew point measurement point with a Vaisala relative humidity probe and a thermistor temperature transducer.

The water vapor injection system has an adjustable pulsed diaphragm pump and a temperature regulated heater. A PID loops controls the evaporation rate to achieve the desired dew point.

The Volatile Organic Compounds reservoir tanks are 5 gallons stainless steel tanks with ¾” FNPT ports. One port allows the deposition of the VOCs on a specially machined Teflon piece using a calibrated syringe. The output of each tank is connected

to two mass flow controllers by Allicat. Three of them are 100sccm and the fourth is 500sccm. The outputs are connected to each Mixing Volume allowing the injection of two distinct compounds to each chamber. The VOCs injection system was put together but not tested.

The ozone generation consists of an ozonator by corona discharge from an old instrument. This connection can be used to inject other gas species.

There are three electrical boxes on the top that provide the control signals for the solenoid pneumatic valves and relays that control the heaters. One box is solely used for input of low voltage signals as the once generated by the thermocouples.

The thermocouple embedded within the heater signal has to be decoupled by connecting on the positive lead of the thermocouple an electrolytic capacitor to remove unwanted 110VAC generated interference. This interference causes the signal to saturate the analog to digital converter not being possible to read the value.

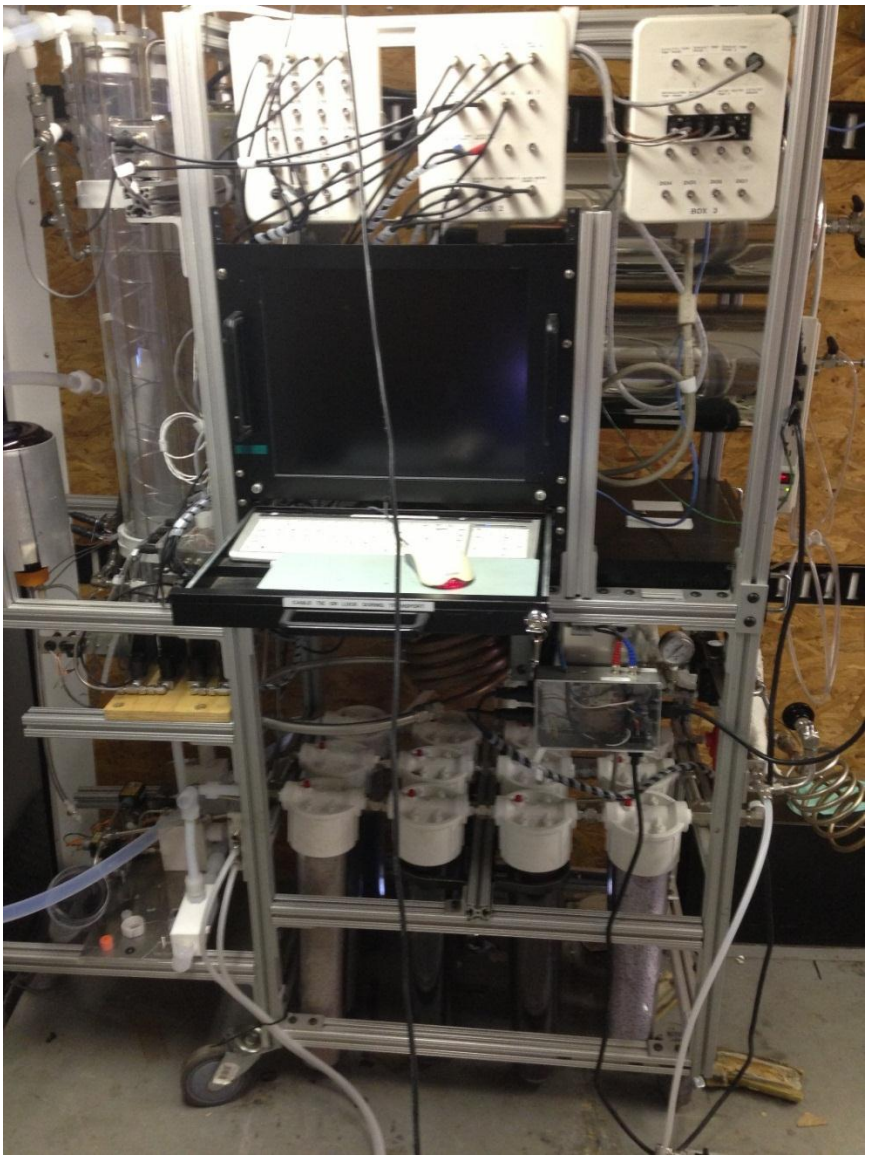

Figure 23. Gas conditioning cart inside the instrumentation trailer.

Figure 23 show the different components of the system. The tall scrubber filters are located at the bottom.

3.8 Compressed air

The compressed air systems consist of a conventional 25 gallons air tank and a Thomas compressor designed for continuous operations. It is located outside the instrumentation trailer. The output from the compressor flows at circa 80psi through a four filter canister, as the previously described scrubbing filters containing silica gel, activated charcoal, potassium permanganate and phosphoric coated charcoal plus two particle filters. After passing through the filters, it flows through a heated tube with catalyst bead -platinum coated aluminum spheres (Shimadzu Corp.) -and it is split into three lines: One feeding the two VOC tanks, a second one feeding a precision pressure regulator set to 30 psi used for the pneumatic Teflon valves on the same cart and the atomizers on the aerosol generation cart and the third line feeding a precision pressure regulator set to 60 psi for the pneumatic valves in the FCC. Figure 24 is a schematic of the compressed air systems.

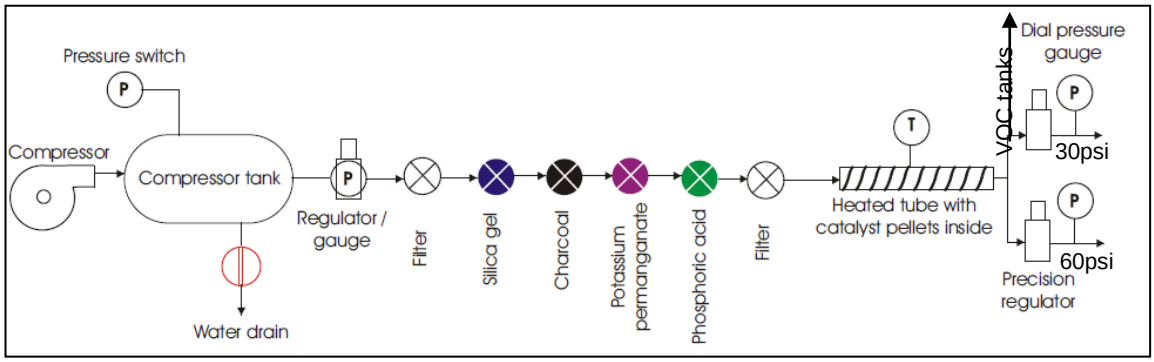

Figure 24. Compressed air schematic

Pneumatic valves were chosen because they do not use any oil for lubrication, thus reducing possible contamination sources into the flows. As with the gas conditioning cart the scrubbing system will have to be replaced periodically.

4. INSTRUMENT OPERATION

While specifying the chamber system for different configuration scenarios, the operation of the instrument turned out to be very similar, regarding the amount of analog input-outputs, digital input-output and the need of using more than computer to a previously built instrument in the research group called the Differential Critical Supersaturation Separator (Osborn 2007). From this experience an alternative path for controlling multiple data acquisition cards and computers was chosen. Given the multiple capabilities of the instrument development of software, using the standard approach was ubiquitous.

The chamber systems have to perform several parallel processes during experiments: sun tracking, chamber rotation, particle injection and air extraction at the same flow rate, recirculation of temperature controlled flow, holding a differential pressure between the concentric volume, etc. All these tasks are controlled by multiple national instrument data acquisition (NIDAQ) cards providing analog inputs (AI) voltage from sensors, generating analog output (AO) voltage to control equipment and digital outputs (DIO).

The numbers of components to control are distributed between the mainframe and the three additional modules namely the flow control cabinet, aerosol generation and gas conditioning cart. Each has a set of NIDAQ in which the channels are linked to the Shared Variable Engine (SVE) which is launched by each computer although only a single computer is used to run experiments with the main software. This approach of

Distributed Control System (DCS) is more similar to what is used in the automation industry than in the aerosol instrumentation community.

These two features of NI LabView software programming allowed a fast development using extensively the Distributed Control System (DSC) and Shared Variable Engine (SVE).

4.1 Distributed control system

Labview DSC module extends the graphical interface by the use of pipe, pump and valve objects converting schematics into a graphical representation of the system flow paths. Several controls were customized to match the schematic valves and components. As it can be seen in the next figure it allowed converting the schematics into the actual instrument real time physical representation.

The figure 25,26 and 27 show the main software tabs that control the entire chamber systems.

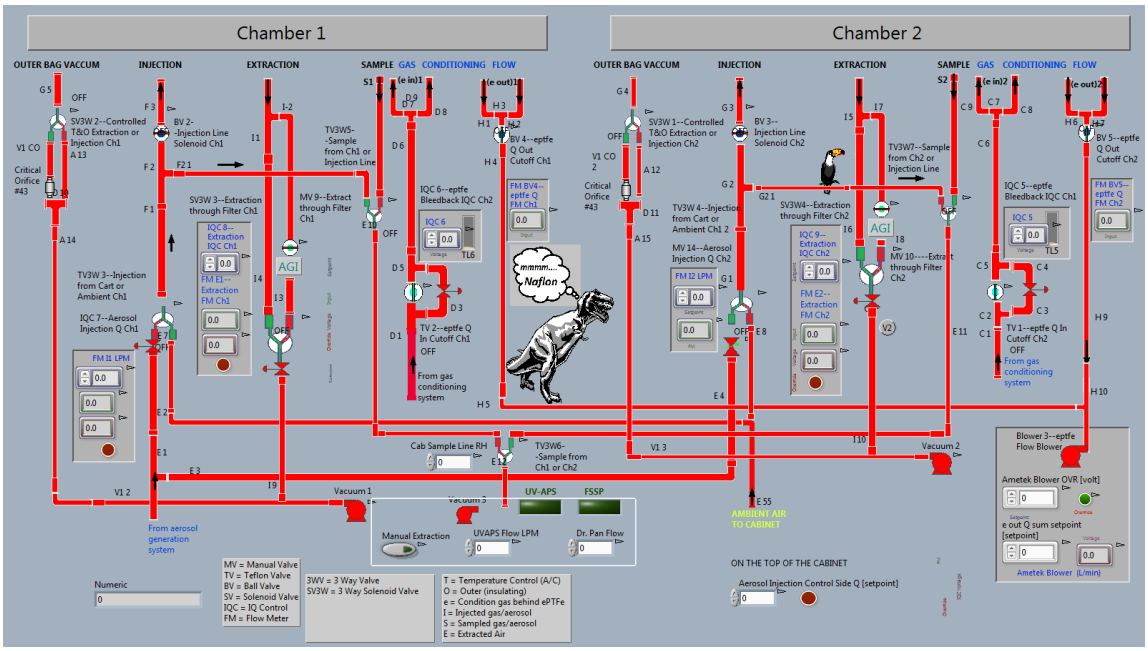

Figure 25. FCC front panel

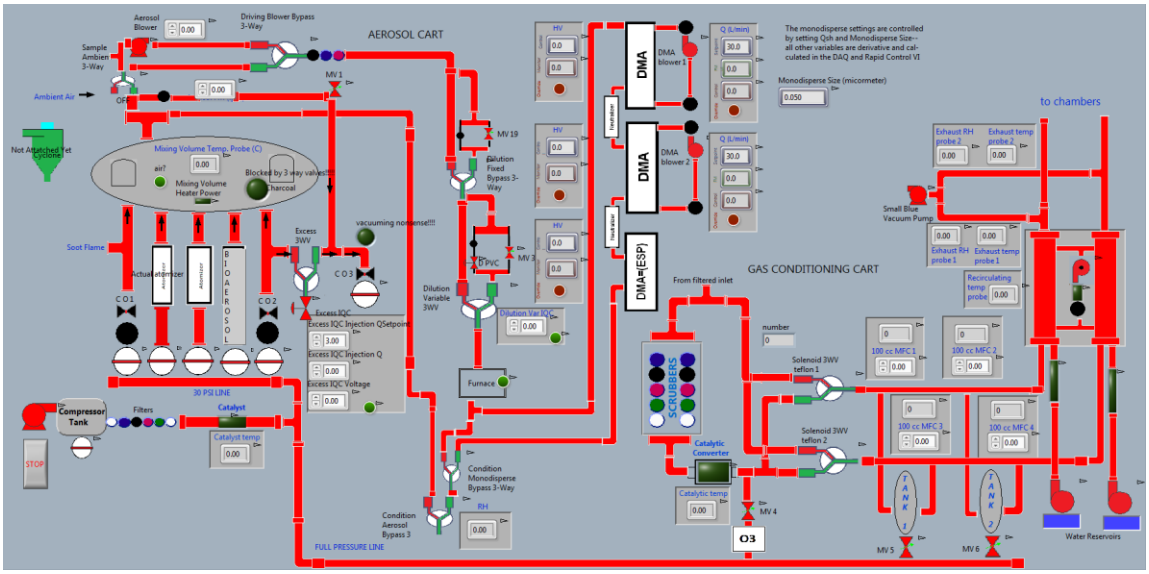

Figure 26. Aerosol generation cart and gas conditioning cart panel

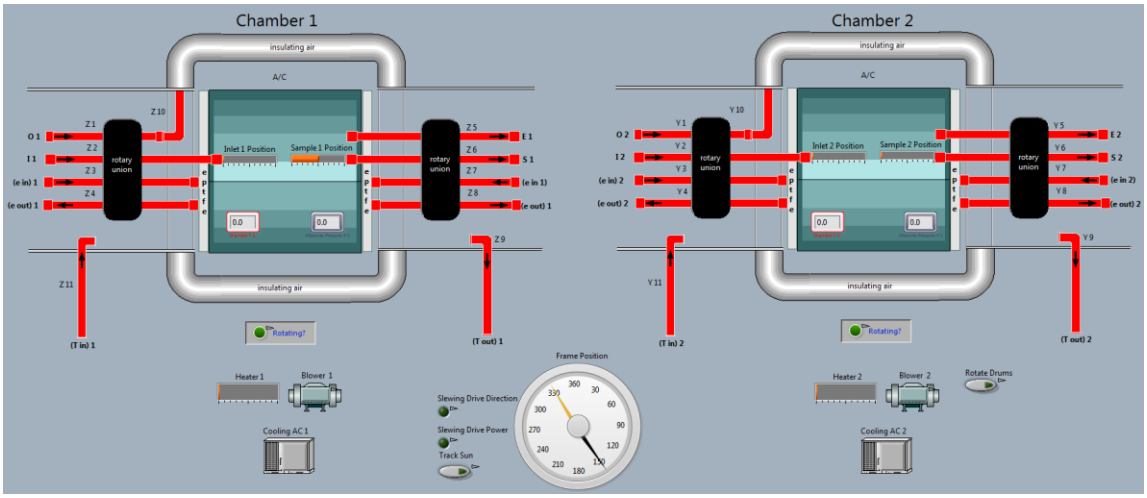

Figure 27. Frame and chambers front panel

Several Virtual Instruments (VI) short code programs run in parallel performing specific task such as analog input reading, analog output and digital output setting, PID flow controls, PID temperature controls. The use of short code programs with only three or four stacked frames facilitates software updates and troubleshooting.

There is a shared variable for every logical and numerical value in the system so that all the small VIs read and write values to the shared variables while the DSC reflects instruments functioning. The main screen is located in the aerosol generation cart which is used as the main computer. This independent real time nonlinear program flow is possible by using the SVE which puts a variable available for reading and writing on the computer network.

For example the gas conditioning flow control system has as inputs the desired flow rate (input text box) and flow rate from the TSI flow meter (analog voltage output) and one output for controlling the blower speed that is an analog voltage controlling the blower. Each of them has an assigned shared variable controlled by some of the small VIs.

Since error signal are also linked to a share variable, any error is used to halt the instruments run and set it into safe operation mode.

Shared variables were grouped together in libraries following the physical distributions. Library names and addresses are launched into arrays in real time providing dynamic access for logging operations and setting from files. As a result, it is very simple to set a configuration for the system, save it and later launch it.

4.2 Multifunction data acquisition

The NIDAQ installed inside the FCC on the trailer has a USB connection for the PC with four slots currently used with an Analog Input, Analog Output and Digital Line modules and a reserved slot for future use. The NIDAQ is controlled by a computer mounted on aerosol generation cart. This NIDAQ controls the FCC and chambers. The FCC has two bulkhead electrical connectors, one is for power and the second one only for control of several solid state relays located inside the electrical cabinet behind the FCC. These solid state relays control the equipment running on 110VAC. Inside the FCC is also a switch box controlling the slewing drive power and direction control.

The Aerosol generation cart computer has 3 NIDAQ cards controlling all the aerosol generation and particle classifier, the three vacuum pumps shown at the bottom of the FCC schematics and compressed air. The gas conditioning cart computer has 3 NIDAQ cards.

4.3 Experimental procedures

Experimental procedures for the chamber systems will depend on the type of project and problem to analyze, the system is very flexible and configuration changes are mainly done in the FCC and Aerosol Cart.

A major advantage of using the ePTFE membrane in the chamber is that the hydroxyl radical concentration will be the same - after a short time lag - in the reactor volume and the ambient air. By using this particle free method for the ambient condition gas transfer the system is run with realistic concentration of this major oxidant.

The chambers are setup with a common starting baseline with same gas-phase composition and environmental characteristics.

It should be noted that the task does not have an estimated duration because this will depend on each type of experiments but field projects will probably use a time span from before dawn to sunset using the transparent, extended retention and sun tracking features of the system. During real time operation monitoring of the systems would occur every hour approximately.

The use of two parallel chambers allows injection of the same aerosol and the observation of changes due to the evolution under different gas species as well the injections of different aerosol types while having an equal gas composition in both chambers.

The aerosol generation particle sizer allows injection of mono disperse size distribution with different mean particle diameter allowing to track individual changes of each injected size distribution. Initially three different nominal sizes of for example 0.01, 0.05 and 0.2μm ammonium sulfate particles will be injected. Each monodisperse population will behave differently under the same gas composition according to the current understanding, providing new information by assessing unique conditions.

The system allows for the modification of one or more variables affecting the aerosol evolution. Using the same aerosol type and modifying different variables one at a time and also all together, the response can be analyzed after performing several experiments. In this way the contribution of single variable that belong to the complex gas composition can be studied.

For Gas perturbation experiments, the chambers are running under identical conditions with the same injected aerosols. After the desired concentration level is measured, one chamber gas exchange system is spiked with the injection of oxidants as O_3 or NO_x, or a trace gas as water vapor increasing RH. Along the experiment duration, periodic samples are taken. This methodology opens the door to studying single effects on the reaction kinetics. Figure 28 shows a typical gas perturbation experiment.

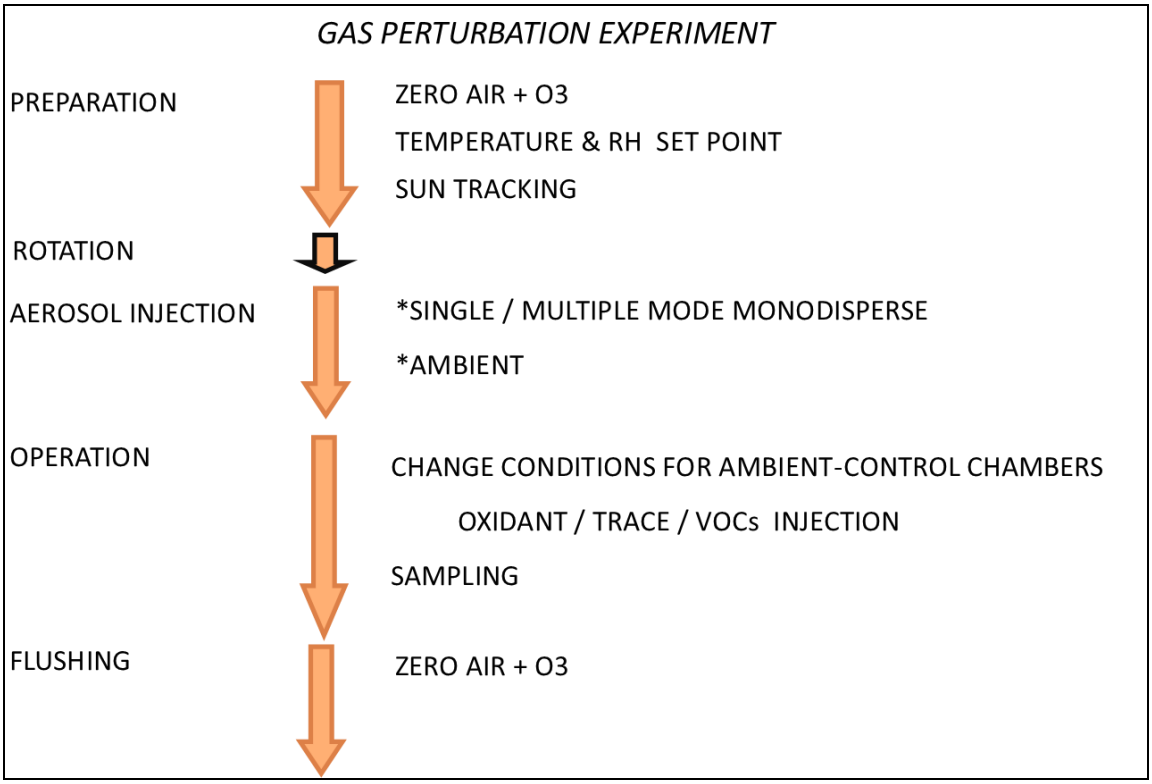

Figure 28. Gas perturbation experiments timing.

For cloud experiments, a unique characteristic of the instruments, the gas conditioning cart will provide an adjustable amount of water vapor into the flow providing a way to increase the relative humidity above ambient prior to the cloud formation process. The pressure reduction required to achieve super saturation will be lower than if starting from ambient relative humidity considerably reducing the total required pressure drop. The wall material deflection will be smaller reducing the long term wrinkling effect. The cooling system adjustable temperature controlled rate should

be able to recreate different up drought velocities changing the adiabatic cooling speed and thus cloud aerosol processing characteristics. Figure 29 shows a typical cloud experiment.

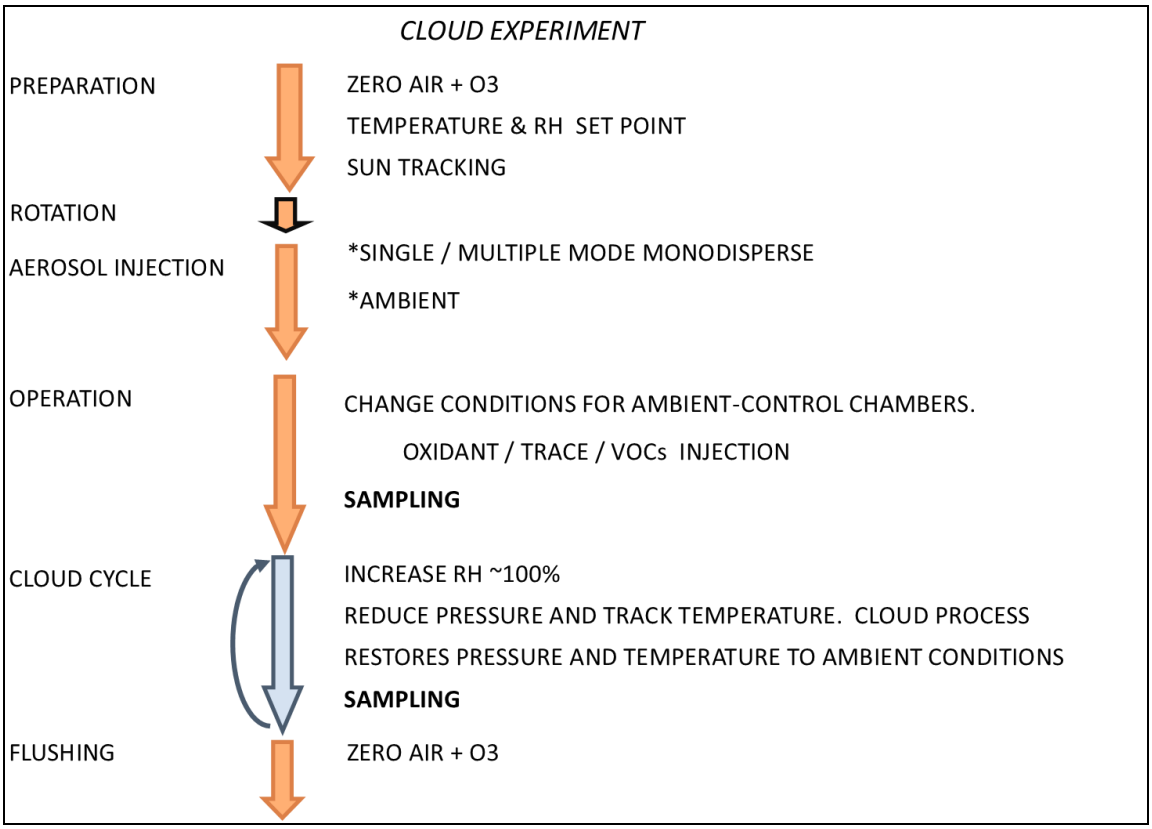

Figure 29. Cloud experiments timing.

During the field campaign (Fall 2012) at the Army Research Laboratory in Adelphi, MD the chambers were tested for the first time. In this experiment a liquid agent was used as the seed aerosol. The setup is outlined in the next figure 30.

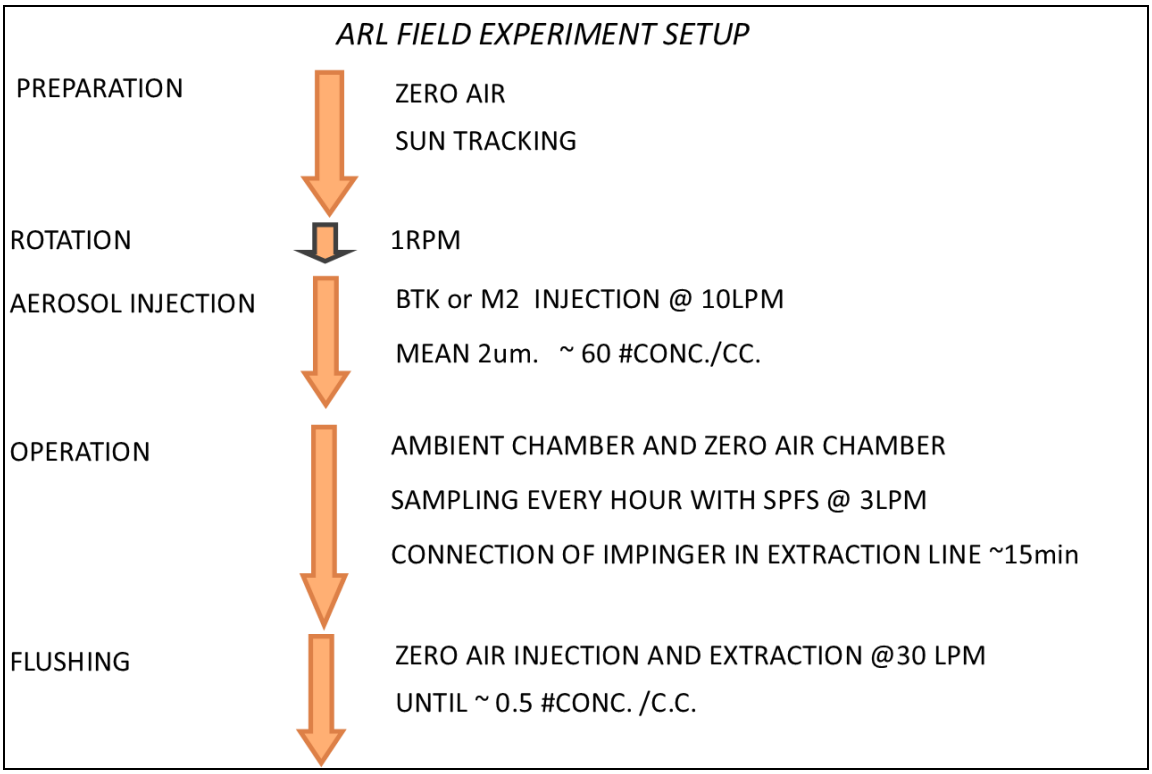

Figure 30. Bioaerosol studies with the chamber timing.

This was the simplest type of experiments along with the system in which one chamber reactor volume contains ambient gas and the other chamber contains zero air gas. A recirculating flow was used to maintain temperature homogeneity and a slight vacuum applied to keep the reactor walls taut. During the experiments ambient ozone concentration and solar intensity were measured.

The FCC is responsible for the actuation of valves and flow balancing of the system. Unfortunately, the variable logging was not ready at the moment of the project but the following figure exemplifies the flow rates and task performed during the experiments that started almost at dawn and finished by sunset. The experiments long duration allowed the aerosol sample exposure to the influence of traffic rush hours anthropogenic gas releases in the atmosphere and its photolysis. The site for experiments is located close to the Capital Beltway (I-495).

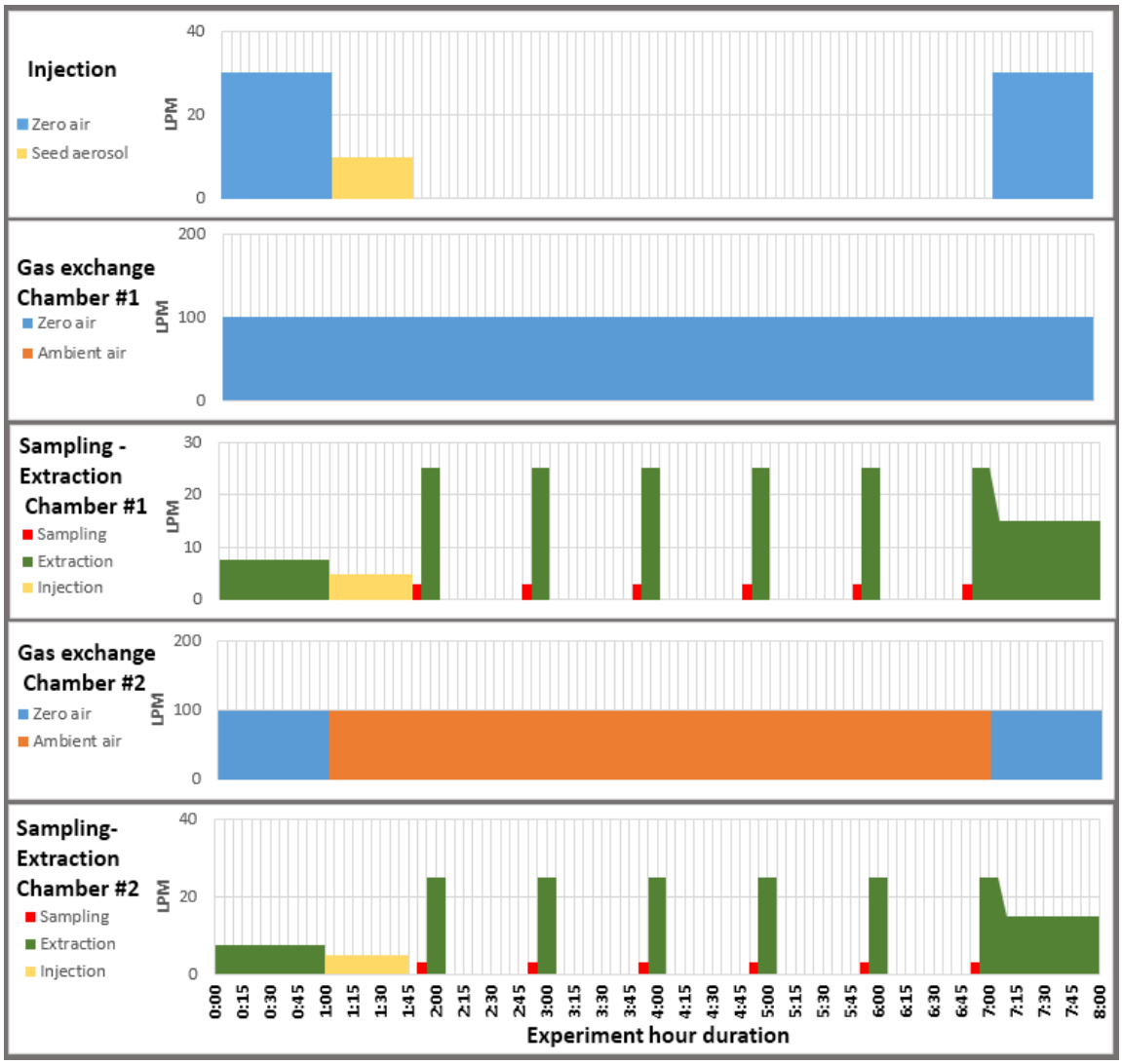

Figure 31. Task timing during 8 hour experiment

Figure 31 shows the events occurring during experiments during an eight hour span.

4.4 Sampling instrumentation

Sampling instrumentation will consist mainly on instrumentation that was built in our group's laboratory and previously used extensively in the field. It includes the Humidified Differential Mobility Analyzer, Aerodynamic Particle Sizer and Cloud Condensation Nuclei counter. Figure 32 shows the instrument sampling configuration for the chambers.

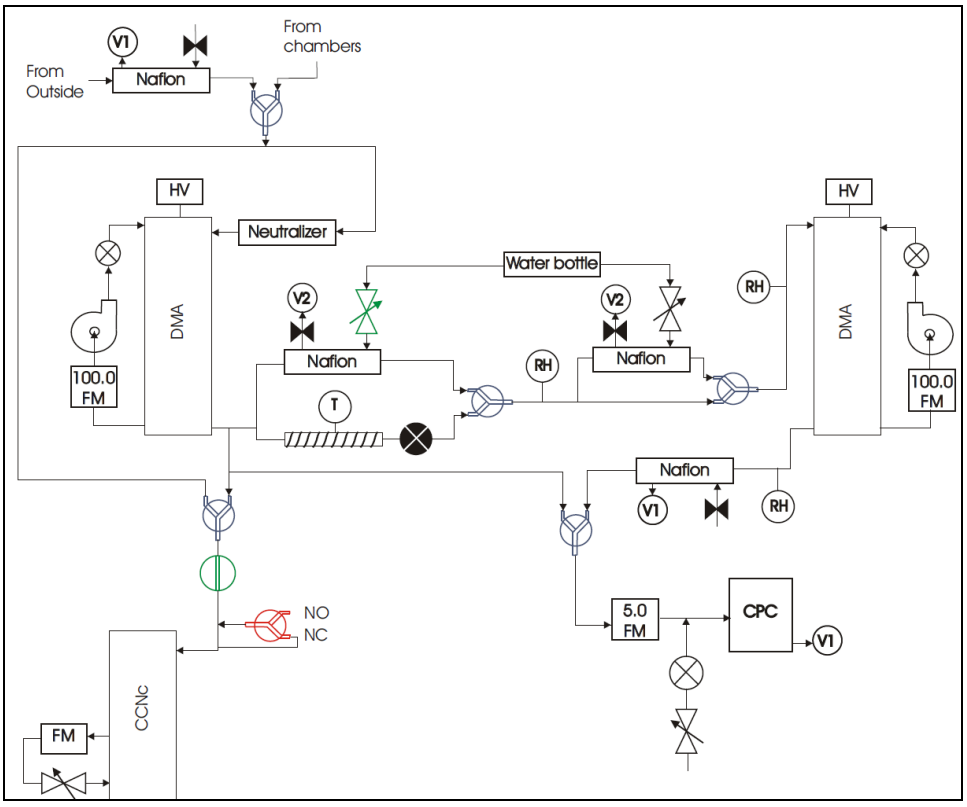

Figure 32. H-TDMA and CCNc configuration for the chambers

For detailed information see Collins et al. (2002) and Gasparini et al. (2006). The instruments provide information of size distribution, hygroscopicity, growth factor and CCN activity.

4.5 Field data

From Sept 27th to Oct 19th, 2012 the systems were finally assembled and experiments were conducted at the US Army Research Laboratory, Adelphi, MD, USA.

Together with researchers from Sandia National Laboratories, John Hopkins Applied Physics Laboratory (JH-APL) and Army Research Laboratory (ARL) experiments were conducted to assess the evolution of aerosol on the outside of a metropolitan city during the summer. For these experiments, one chamber was used with ambient supplied air from the gas exchange systems while the second used clean air.

Two different types of seed aerosols were used which are simulants of biological compounds with a mean diameter of nearly 2μm.

Some biological molecule fluorescence, after being illuminated with a laser at a fix wavelength and the fluorescence spectral measurement results can be used to identify biological compounds.

The JH-APL research group made aerodynamic size distribution and ultra violet fluorescence measurement with a TSI UV-APS, and ARL made single particle fluorescence spectra measurements with a dual excitation wavelength single particle spectrometer (SPFS) fixed at 263nm and 351nm.

Throughout the experiments, both chambers were rotating at around 1 r.p.m. and particle concentration decay was faster than expected having experiments an approximately 6 hours span. Initial particle concentration was varied between 60~120 particles per cubic centimeter measured with the UV-APS and particle e-folding time was averaged to be 153 minutes. Figure 33 depicts the instrumentation setup.

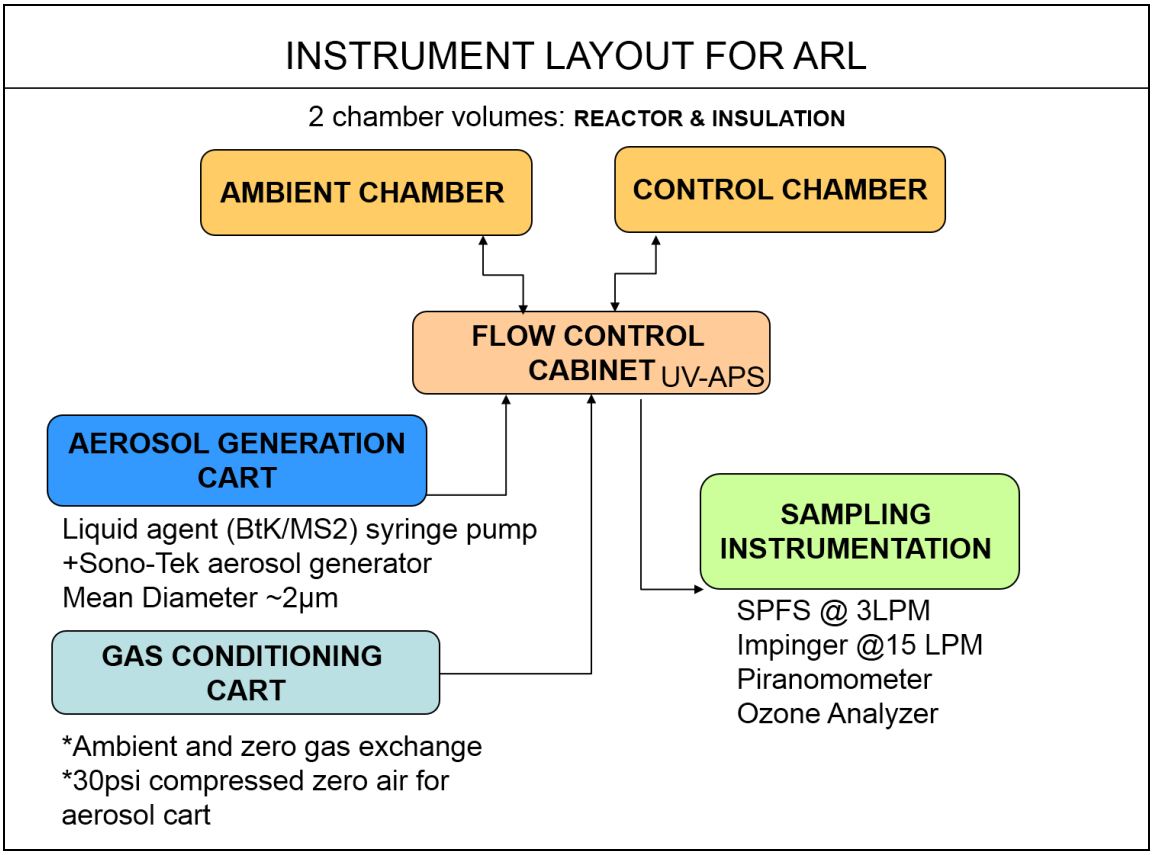

Figure 33. Instrument setup for ARL

During the experiments the chamber configuration had two of the three chamber walls using only the reactor volume and outer insulating volume. The outer volume conditions had the recirculating blowers turned on and a controlled vacuum was applied which pulled the reactor volume bag taut. The adjustable temperature system was not installed yet and the system was tracking ambient temperature and relative humidity.

In this configuration, the particle decay could be explained due to a differential pressure between both gas exchange walls. At a flow rate of 100LPM, the pressure drop in tubing is significant and the tubing lines from the cabinet towards the gas exchange systems are not equal by 10 feet approximately. As the lowest pressure is on the inlet side, airflow will be constant towards that wall reducing concentration on the sampling outlet side. Also as the reactor volume has positive pressure, a bad seal would leak particles and air to the outside without causing any bag deflation as particle free air is continuously supplied by the gas exchange system.

Data from October 18th is presented. It was a sunny day with both chambers running. Samples were taken form one chamber first and immediately afterwards from the second chamber. Once the flow was routed towards the instrumentation, it took around a minute to have the first signal from SPFS instrument located in the trailer while data on the UV-APS located in the cabinet took a few seconds. The following figure shows the typical concentration decay seen throughout the experiments. MS2 is the name of the seed aerosol used which contains biological molecules fluorescing to UV laser excitation allowing for its detection.

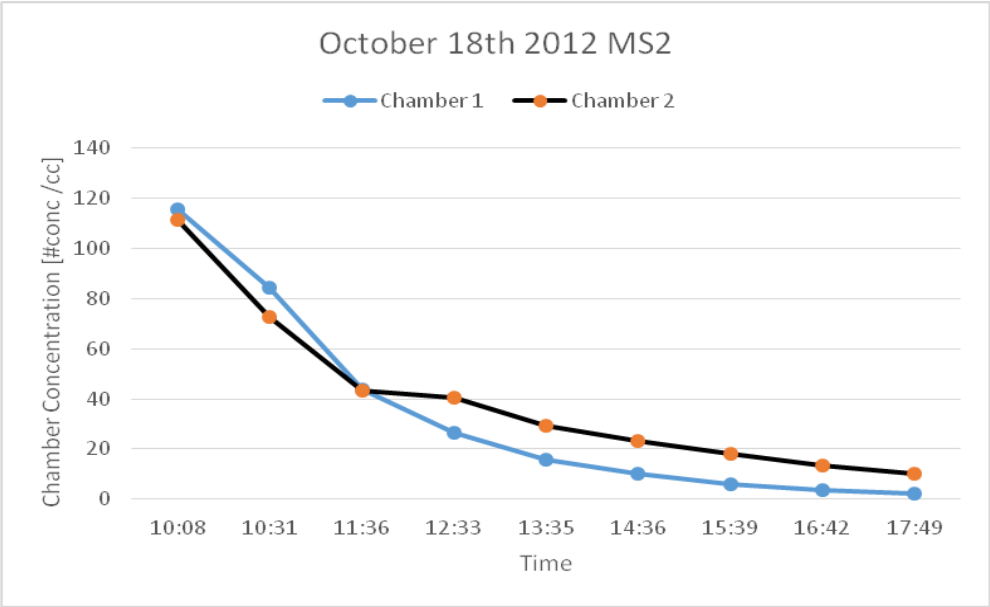

Figure 34. Particle concentration decay

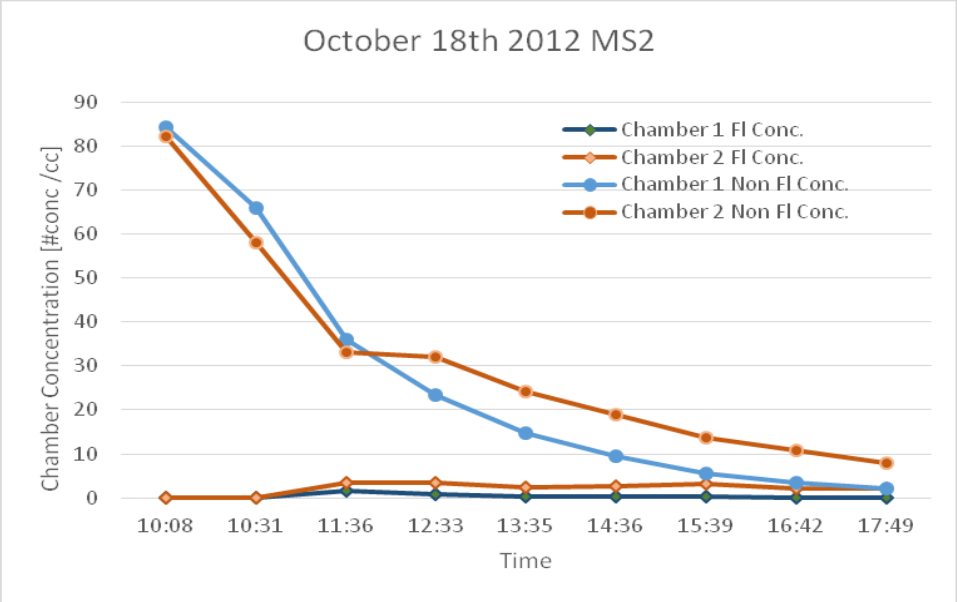

Figure 35. Instrument particle fluorescence and non-fluorescence concentration

Figure 35 shows the different concentration level of particles with fluorescence and non-fluorescence characteristics during the experiment. Figure 36 and 37 show the results from the SPFS for the chambers where fluorescence intensity has been normalized by particle size [$I/(d)^{2.08}$]. The figures were provided by Dr. Yong-Le Pan.

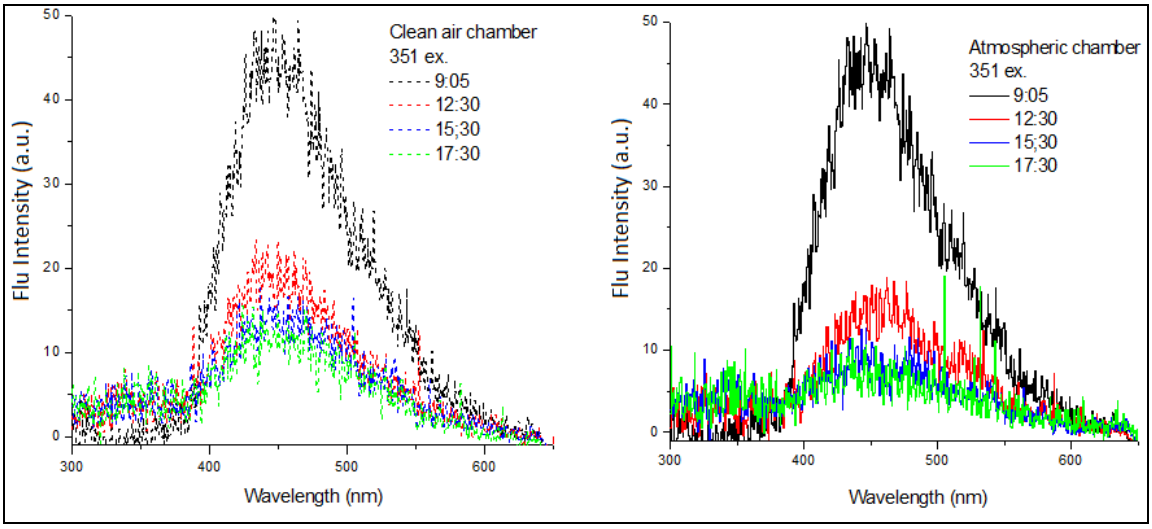

Figure 36. SPFS spectral measurement for the 351m excitation laser.

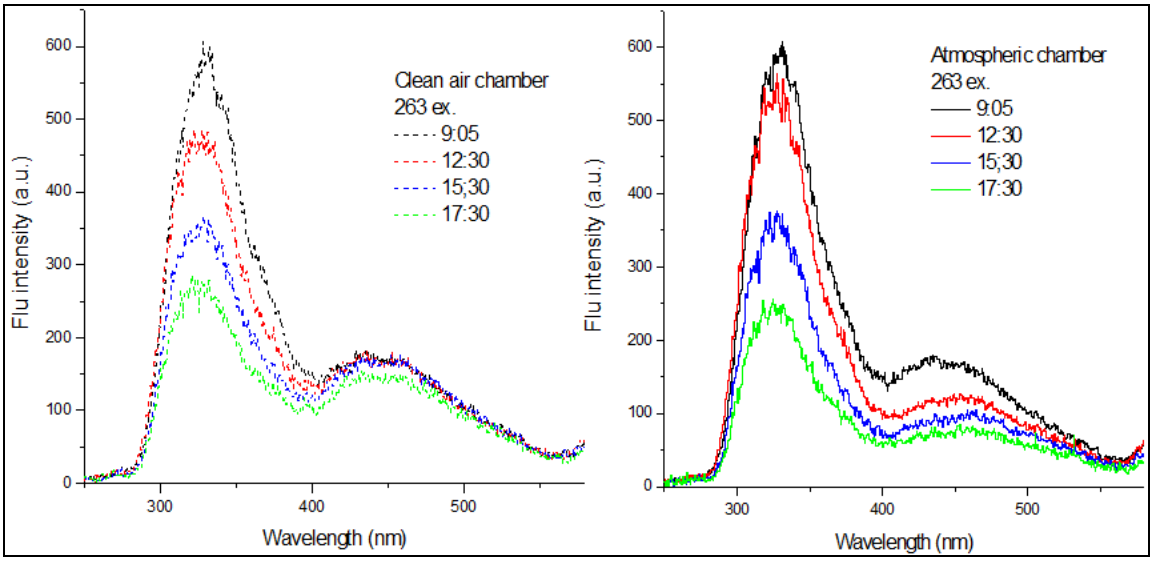

Figure 37. SPFS spectral measurement for the 263nm excitation laser

Fluorescence spectral profile and intensity varies with time differently in both chambers while using a different gas composition which is the only environmental variable that was adjusted for the experiments demonstrating the influence of gas composition effect on the seed aerosol. It can be seen for both laser wavelength a change during the day in the profile in the 400 to 500nm range.

The instruments were put to work together for the first time and experiments conducted with the assistance and collaboration of Yong-Le Pan, Steve Hill and Mark Coleman from the US Army Research Laboratory; Shanna Ratnesar-Shumate, Christopher Bare and Sean Kinahan from the Johns Hopkins University Applied Physics Laboratory and Andres Sanchez, Crystal Reed and Joshua Santarpia from Sandia National Laboratories. Dr. Don Collins, principal investigator of the Aerosol Research

Group, and research assistants Jill Matus, Nathan Taylor and myself from Texas A&M University.

5. SUMMARY AND CONCLUSIONS

The chamber systems which were developed provides a deployable instrument for measurements of captive aerosol in situ conditions, of special interest to study the evolution with daily fluctuating concentration levels of gas and particles as physical environmental conditions leading to the study of intraday variations. This kind of experiments complements laboratory measurements in which a single parameter is usually modified with the purpose of isolating effects.

During the fall of 2012 from Sept 27th to Oct 19th, 2012 at US Army Research Laboratory, Adelphi, MD, USA providing the first set of data made with the instrument to study the UV-laser-induced fluorescence spectra and viability of bioaerosols and its possible correlations between the changes in aerosol properties and the environmental conditions.

The design of an instrument to measure the effect of atmospheric conditions, - including gases, sunlight, and humidity, and in the future, aqueous phase chemistry- proved to be a challenge for the unknown response of the equipment and the various accompanying modules required to make it work in a consistent manner experiment after experiment. Together with the quantity of power and signals, moveable pieces and constraint for the design; each electrical, pneumatic or mechanical assembly had to be tested and modified until the desired outcome was obtained which was hardly ever achieved at a first attempt.

A consideration for the system is to have a test point that will allow the checking of voltages both read and generated by the NIDaq.

This design still needs to be tested for characterization purposes. The next set of planned measurements will be on contamination issues and pursuing cloud formation by adiabatic cooling.

Results were shown during the American Association for Aerosol Research 32nd annual conference from September 30 to October 4 2013 in Portland, Oregon.

REFERENCES

Aitken, J. (1880a): “On Dust, Fogs and Clouds”. Proc. R. Soc. 11:14-18.

Aitken, J. (1880b): “On Dust, Fogs and Clouds”. Nature: 384-385.

Caffrey, P., et al. (2001): “In-Cloud Oxidation of SO2 by O3 and H2O2: Cloud Chamber Measurements and Modeling of Particle Growth”, Journal Geophysical Research, 106(D21), 27587–27601, doi: 10.1029/2000JD900844.

Carter, W. P. L., Luo, D., Malkina, I. L. and Fitz, D.: (1995). “The University of California, Riverside Environmental Chamber Data Base for Evaluating Oxidant Mechanisms - Indoor Chamber Experiments Through 1993”, U.S. Environment Protection Agency, 240.

Carter, W. P. L. , Cocker III, D. R., Fitz, D. R. , Malkina, I. L., Bumiller, K., Sauer, C. G., Pisano, J. T. ,Bufalino, C. , and Chen Song: (2005). "A New Environmental Chamber for Evaluation of Gas-Phase Chemical Mechanisms and Secondary Aerosol Formation”, Atmospheric Environment, 39 7768–7788.

Collins, D. R., Flagan, R. C., Seinfeld, J. (2002): H. “Improved Inversion of Scanning DMA Data”, Aerosol Science and Technology, 36:1, 1-9, doi: 10.1080/027868202753339032.

Cocker, D.R., Flagan, R.C., Seinfeld, J.H.: (2001a).”State-of-the-Art Chamber Facility for Studying Atmospheric Aerosol Chemistry”. Environmental Science Technololgy, 35, 2594–2601.

Gasparini, R., Collins, D. R., Andrews, E., Sheridan, P. J. , Ogren, J. A. and Hudson, J. G. (2006): “Coupling Aerosol Size Distributions and Size-Resolved

Hygroscopicity to Predict Humidity-Dependent Optical Properties and Cloud Condensation Nuclei Spectra", Journal Geophysical Research.-Atmos. 111: art. No. D05S12.

Goldberg, L. J. , Watkins, H. M. S. , Boerke,E. E and Chatigny, M. A. (1958): "The Use of a Rotating Drum for the Study of Aerosols over Extended Periods of Time", American Journal of Epidemiology 68(1): 85-93.

Goldstein, A.H. and Galbally, I.E. (2007): "Known and Unexplored Organic Constituents in the Earth's Atmosphere", Environmental Science Technology, 41,1514-1521.

Gruel, R. L., C. R. Reid, R. T. Allemann (1987): "The Optimum Rate of Drum Rotation for Aerosol Aging", Journal of Aerosol Science 18(1): 17-22.

Hallquist, M., Wenger, J. C., Baltensperger, U. , Rudich, Y. , Simpson, D., Claeys, M., Dommen, J., Donahue, N. M., George,C. , Goldstein, A. H. , Hamilton, J. F. , Herrmann,H. , Hoffmann, T., Iinuma,Y. , Jang, M. , Jenkin,M. E. , Jimenez, J. L. , Kiendler-Scharr, A. , Maenhaut,W. , McFiggans,G. , Mentel, T. F. , Monod, A. , Prévôt,A. S. H. , Seinfeld, J. H. , Surratt, J. D. , Szmigielski, R. and Wildt, J. (2009): "The Formation, Properties and Impact of Secondary Organic Aerosol: Current and Emerging Issues", Atmospheric Chemistry Physics, 9(14): 5155-5236.

IPCC (2007): Summary for Policymakers, in: Solomon, S., D. Qin, et al. (Eds.), Climate Change 2007: "The Physical Science Basis. Contribution of Working Group I to

the Fourth Assessment Report of the Intergovernmental Panel on Climate Change", Cambridge University Press, New York.

Krumins, V., Son, E.K., Mainelis, G. and Fennell, D. E. (2008): "Retention of Inactivated Bioaerosols and Ethene in a Rotating Bioreactor Constructed for Bioaerosol Activity Studies", CLEAN – Soil, Air, Water 36(7): 593-600.

McMurry, P. H. & Rader, D. J. (1985): "Aerosol Wall Losses in Electrically Charged Chambers", Aerosol Science and Technology, 4:3, 249-268.

Taylor, N. F., Collins, D. R., Spencer, C. W., Lowenthal, D. H., Zielinska, B., Samburova, V., and Kumar, N. (2011): "Measurement of Ambient Aerosol Hydration State at Great Smoky Mountains National Park in the Southeastern United States", Atmospheric Chemistry Physics, 11, 12085-12170, doi:10.5194/acp-11-12085-2011.

Weitkamp, E. A., Sage, A.M., Pierce, J.R., Donahue, N.M. and Robinson, A. L. (2007): "Organic Aerosol Formation from Photochemical Oxidation of Diesel Exhaust in a Smog Chamber", Environmental Science Technology, 41, 6969-6975, doi: 10.1021/es070193r.